Regulation of Nitrate-N Release From Temperate Forests: A Test of the N Flushing Hypothesis

Article *in* Water Resources Research · November 1996

DOI: 10.1029/96WR02399

7 authors, including:

Irena F Creed
University of Toronto
273 PUBLICATIONS **12,439** CITATIONS
SEE PROFILE

L. E. Band
University of North Carolina at Chapel Hill
172 PUBLICATIONS **14,379** CITATIONS
SEE PROFILE

Dean Jeffries
Government of Canada, Department of Environment and Climate Change, Burlingto…
106 PUBLICATIONS **6,867** CITATIONS
SEE PROFILE

WATER RESOURCES RESEARCH, VOL. 32, NO. 11, PAGES 3337–3354, NOVEMBER 1996

Regulation of nitrate-N release from temperate forests: A test of the N flushing hypothesis

I. F. Creed and L. E. Band

Department of Geography, University of Toronto, Toronto, Ontario, Canada

N. W. Foster, I. K. Morrison, and J. A. Nicolson

Forestry Canada, Great Lakes Forestry Centre, Sault Sainte Marie, Ontario, Canada

R. S. Semkin and D. S. Jeffries

Environment Canada, Canada Centre for Inland Waters, Burlington, Ontario, Canada

Abstract. During the past decade, significant spatial and temporal variability in the release of nitrate-nitrogen (N) from catchments in a sugar maple forest in central Ontario was observed. To explain this variability, we tested the flushing hypothesis [*Hornberger et al*., 1994], where, when the soil saturation deficit is high, N accumulates in the upper layers of the soil and, as the soil saturation deficit decreases, the formation of a saturated subsurface layer flushes N from the upper layers of the soil into the stream. We used the Regional Hydro-Ecological Simulation System to simulate water, carbon, and N dynamics. A N flushing index was modeled as S/S_{30}, the ratio of the current day saturation deficit to the previous 30-day average saturation deficit. A N source index was modeled as the ratio of N supply/demand. The relationship between the simulated N indices and the observed release of N indicated two mechanisms for the release of N from catchments: (1) a N flushing mechanism, where the N-enriched upper layer of the soil is flushed, after a period of low demand for N by the forest (e.g., during spring snowmelt and autumn stormflow, the water table rising into previously unsaturated parts of a N-enriched soil profile) or after a period of high demand for N by the forest (e.g., during summer droughts, the water table rising into previously saturated parts of a N-impoverished soil profile following a period of enhanced rates of nitrification); and (2) a N draining mechanism, where spring snowmelt recharge of the groundwater translocates N from the upper layer of the soil into deeper hydrological flow pathways that are released slowly over the year.

1. Introduction

Environmental perturbations may lead to changes in the character of nitrate-nitrogen export to waterways, thereby reducing water quality. To facilitate proper management of the aquatic resources, we must advance our understanding of the sources of nitrogen species from within the landscape, of the mechanisms that lead to the export of the nitrogen species, and of the concentrations and fluxes of each nitrogen species being exported from the landscape. This paper explains the timing and magnitude of nitrate-nitrogen (N) release from a humid, temperate, forested catchment.

There is substantial temporal heterogeneity in the flows of N within landscapes [*Vitousek and Reiners*, 1975; *Nicolson*, 1988, 1991; *Semkin et al*., 1984; *Aber et al*., 1989; *Stoddard*, 1994]. The ability to predict the character of these flows is important, as it leads to the potential to predict the impacts of imposed environmental changes that significantly alter the character of N flows. For example, elevated levels of atmospheric N deposition to a forest will result in fundamental changes in the flows of N as the catchment undergoes a transition from an anticipated net sink of N (N-limited forest) to a net source of N (N-enriched forest) [*Stoddard*, 1994]. These changes in the character of the flows of N will have important environmental implications both in terms of the potential land-air and land-lake biogeochemical exchanges within the landscape and in terms of the potential productive capacity of the landscape.

For prediction of biogeochemical fluxes (e.g., dissolved organic carbon (DOC) and N) across land-lentic and land-lotic interfaces within the landscape, catchments become the basic modeling units. As water flows through the catchment, the alteration of its chemical composition may occur in a predictable manner according to known physical, biological, and chemical equilibrium processes [*Carpenter et al*., 1995]. The extent to which the chemical composition is altered is a reflection of the exposure of the water to chemically altering environments. Topography, through its gravitational effects, influences the creation of these chemically altering environments as well as the pathway of water flowing through these chemically altering environments. The topographic effect on the pathway of water flows is considered in a topographically based hydrology model (Topmodel) [*Beven and Kirkby*, 1979]. Topmodel has been used to compute streamflow and to partition streamflow into its sources, including overland, shallow subsurface, and deep subsurface flow pathways [*Wolock et al*., 1990; *Robson et al*., 1992; *Hornberger et al*., 1994]. When combined with a simple mixing model, Topmodel has also been used to compute the temporal changes in both conservative substances

Paper number 96WR02399.
0043-1397/96/96WR-02399$09.00

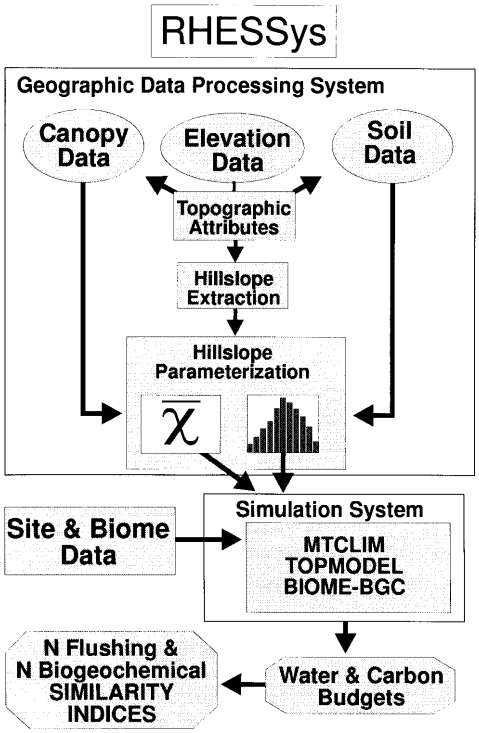

Figure 1. A schematic diagram of the Regional HydroEcological Simulation System (RHESSys). The engine of RHESSys is the simulation system. Inputs to the simulation system include site and biome parameters and for each hillslope within the landscape the average and frequency distribution of climate, topography, soils, and canopy parameters. Outputs from the simulation system include biogeochemical budgets, from which are derived the N flushing and N biogeochemical indices.

[*Robson and Neal*, 1991] and, once the source and sink terms of the nonconservative substances have been represented, nonconservative substances [*Hornberger et al*., 1994].

Previous studies have postulated a topographically based flushing mechanism to describe the major features of the temporal variation in the concentration of biogeochemical solutes in streams [e.g., *Hornberger et al*., 1994]. The characteristic peak in the concentration of biogeochemical solutes in the discharge that occurs prior to the peak in discharge has been termed the "flushing effect" [*Edwards*, 1973; *Walling*, 1974; *Walling and Foster*, 1975]. The conceptual basis of the flushing effect is that biogeochemical solutes in soils are flushed to the stream by the formation of a rising water table during snowmelt or stormflow [*Hornberger et al*., 1994]. For example, the flushing effect has been suggested to explain the relationship of DOC concentration to discharge based on field-based studies [*Lewis and Grant*, 1979; *Foster and Grieve*, 1982; *Fiebig et al*., 1990; *Baron et al*., 1991; *Denning et al*., 1991; *Boyer et al*., 1995] and model-based studies [*Hornberger et al*., 1994; *Boyer et al*., 1996]. The flushing effect has also been suggested to explain the observed relationship of N concentration to discharge [*Murdoch and Stoddard*, 1992; *Stoddard*, 1994].

The present study builds on previous work by modeling and testing the flushing effect for N. Our formalization of the flushing effect is similar to that described by *Hornberger et al*. [1994] in terms of using the topographically influenced hydrological flow pathways (via Topmodel) to predict when and from where in the catchment the reservoir of N in the soil is flushed. However, testing the flushing effect for N has an added complexity as catchments undergo temporal shifts from being a sink or source of N. We use a distributed hydroecological model which couples Topmodel to a forest biogeochemical model to test the flushing mechanism for N.

The goal of our research is to develop an understanding of the topographic controls on the N cycling and routing flow pathways within the Turkey Lakes Watershed, in central Ontario, Canada. The objectives of this paper are the following: (1) to determine if the simulated soil saturation deficit and its oscillations can be correlated to the observed release of N into adjacent waters, implicating the dominant hydrological mechanism controlling the release of N; and (2) to determine the importance of the timing of the flushing in a catchment that undergoes temporal shifts in its functional states (i.e., a sink versus a source of N) over the seasonal cycle.

To achieve our objectives, we use a "hybrid" indicator approach, in which we derive indices of the simulated catchment processes (including indices of the catchment's N flushing and N biogeochemical activities) and relate them to the observed release of N to the stream. We do not simulate the release of N to the stream. The indices are simplified representations of the underlying physics of the catchment processes which still capture the emergent biogeochemical behavior of the catchment system, and therefore the indices allow for the general application of this approach to other catchments.

2. Modeling Approach

The Regional HydroEcological Simulation System (RHESSys) is a spatial data processing and simulation system designed to compute spatially distributed biogeochemical stores and fluxes within landscapes (10^1–10^3 km^2) (Figure 1).

The landscape is partitioned into a population of discrete land units, defined to (1) minimize the within-unit variance and (2) maximize the between-unit variance of model parameters. In landscapes where topography (e.g., surface slope, aspect, elevation) has an influence on the biogeochemical storage and flux variables, hillslopes are chosen as the basic modeling land unit. Simulation of biogeochemical processes over the population of hillslopes captures the dominant variability in the biogeochemical processes within the landscape [*Band et al*., 1991, 1993].

For each hillslope the simulation system computes the meteorological driving variables (MTCLIM), a one-dimensional carbon and water budget (Forest-BGC), and a three-dimensional redistribution of the water budget (Topmodel).

2.1. Microclimate Simulator: MTCLIM

Meteorological inputs are altered in response to variations in topographic features. To optimize the inputs to the simulation system, meteorological variables must be extrapolated from the meteorological recording station to each hillslope. Within MTCLIM [*Running et al*., 1987], a combination of algorithms is used to calculate the hillslope-specific meteorological variables:

1. Potential incoming shortwave radiation is based on the original algorithm for a flat surface that is modified by latitude, slope, aspect [*Garnier and Ohmura*, 1968], and atmospheric transmissivity [*Bristow and Campbell*, 1984].
2. Below canopy air temperature is adjusted by the eleva-

tional adiabatic lapse rate and the attenuation of incoming short-wave radiation through the canopy based on Beer's law.

3. Humidity is based on the algorithm of *Murray* [1967] which combines air temperature and dew point temperature to derive daily averages of humidity.

4. Precipitation that is measured at the meteorological recording station is adjusted using the isohyetal method (i.e., ratio of annual isohyets of the hillslope relative to the station).

The model is run on a daily time step, corresponding to the timing of available meteorological records.

2.2. Biogeochemical Simulator: Forest-BGC

Using the hillslope-specific meteorological inputs, Forest-BGC [*Running and Coughlan*, 1988] calculates water and carbon stores and fluxes.

Canopy and litter interception are treated as simple bucket models with set capacities.

The water flux terms for canopy and litter evaporation are a function of the absorbed short-wave radiation and the vapor pressure deficit.

The water flux term for canopy transpiration is computed using the Penman-Monteith equation (T, m^2 d^{-1}) [*Monteith*, 1965]:

$$T = \left[\frac{\Delta Q_n + c_p \rho_a g_a \,\mathrm{VPD}}{\Delta + \gamma\left(1 + \frac{g_a}{g_c}\right)} \right] \frac{\mathrm{DL}}{\rho_w \,\mathrm{LE}} \tag{1}$$

T canopy transpiration, m^2 d^{-1}.
Δ slope of the saturation vapor pressure curve at ambient air temperature, mbar °C^{-1}.
Q_n net all-wave radiation, J m^{-2} s^{-1}.
c_p specific heat of air, J kg^{-1} °C^{-1}.
ρ_a density of air, kg m^{-3}.
g_a canopy H_2O aerodynamic conductance, m s^{-1}.
g_c canopy H_2O stomatal conductance, m s^{-1} (the canopy stomatal conductance is resolved as a function of incident photosynthetically active radiation (PAR), air temperature, vapor pressure deficit, and soil water content).
VPD vapor pressure deficit from canopy to air, mbar.
γ psychrometric constant, mbar °C^{-1}.
DL day length, s d^{-1}.
ρ_w density of water, kg m^{-3}.
LE latent heat of vaporization of water, J kg^{-1}.

The carbon flux term for canopy photosynthesis (PSN, kg C m^{-2} d^{-1}) [*Lohammer et al*., 1980] is estimated by

$$\mathrm{PSN} = \left[\frac{\Delta\ \mathrm{CO_2}\, c g_c g_m}{g_c + g_m} \right] \mathrm{LAI} \cdot \mathrm{DL} \tag{2}$$

PSN canopy photosynthesis, kg C m^{-2} d^{-1}.
ΔCO_2 CO_2 diffusion gradient from leaf to air, kg CO_2 m^{-3}.
c CO_2/H_2O diffusion correction, dimensionless.
g_m canopy CO_2 mesophyll conductance, calculated from light, temperature, and nitrogen functions that modify a prespecified maximum canopy CO_2 mesophyll conductance, m s^{-1}.
LAI leaf area index, m^2 m^{-2}.

while the carbon flux term for canopy, stem, and root maintenance respiration (RESP) is based on the respiring biomass and the air temperature [*Running and Coughlan*, 1988].

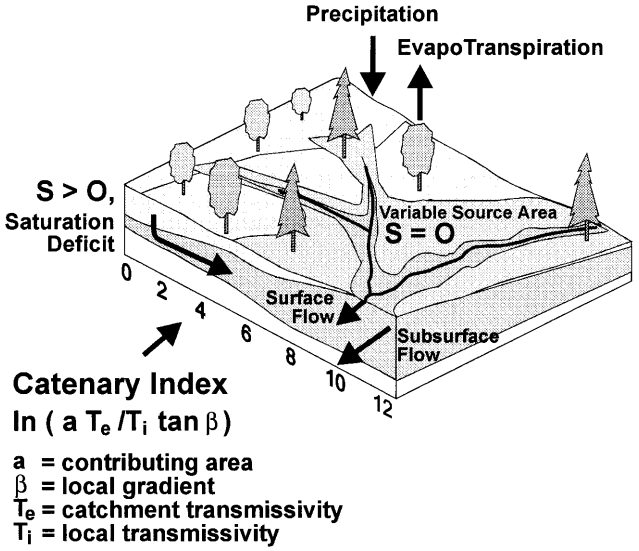

Figure 2. A schematic of Topmodel, a topographically-based hydrology model (modified after *Hornberger et al*. [1985]). In Topmodel a catenary index [ln (aT_e/T_i tan β)] is used to simulate the catchment's distribution of soil water saturation deficits S, which form the basis of the flushing mechanism.

Daily net carbon fixation (PSN − RESP) is summed throughout the year. At the end of the year, a static allocation fraction of net carbon to the forest structural compartments is made (e.g., 0.25, 0.35, and 0.40 for canopy, stem, and root, respectively). Additional information on the biogeochemical process computations can be found in the work by *Running and Coughlan* [1988], *Running and Gower* [1991], and *Running and Hunt* [1993].

2.3. Hydrological Simulator: Topmodel

The water and carbon flux rates are strongly influenced by the availability of water within the landscape. In Forest-BGC the biogeochemical processes are one-dimensional. *Band et al*. [1993] coupled Forest-BGC with a hillslope hydrology model, Topmodel (Figure 2), to enable the distribution of the biogeochemical processes over the three-dimensional landscape.

For each hillslope in the landscape we compute the daily soil saturation deficit S_h based on the following water balance equation:

$$S_h = S_p - R_n + O \tag{3}$$

S_h hillslope-average soil saturation deficit, m.
S_p previous day hillslope-average soil saturation deficit, m.
R_n net recharge to the saturated zone, a function of the precipitation or melt that exceeds the interception capacity of the litter and the unsaturated soil water dynamics as computed by Forest-BGC, m.
O subsurface discharge, m.

Soil saturation occurs when all the soil pores are filled with water. The soil saturation deficit is the amount of additional water required to fill all of the pores. Although the soil saturation deficit scale is represented as a positive scale throughout this manuscript, it is really a negative scale.

The local soil saturation deficit is dependent on its catenary position within the hillslope. Typically, positions with larger contributing drainage areas and lower surface slopes (i.e., near

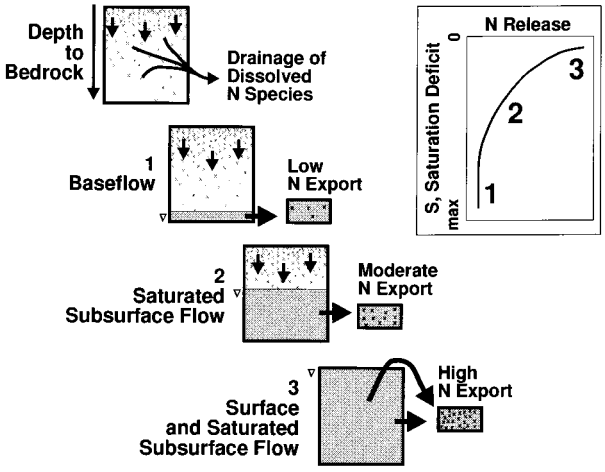

Figure 3. A schematic of the flushing hypothesis. The conceptual basis for the flushing hypothesis is represented in the three stages of N release from the catchment. Each box represents a soil profile. In each box the crosses represent dissolved N species in the soil profile. The concentration of dissolved N species is higher in the upper portion of the soil profile and declines through the soil profile as there is a decline in the N transformation rates. The flushing hypothesis predicts an exponential increase in the release of N as the saturation deficit decreases: At stage 1, when the saturation deficit is high, there is a low release of N from the catchment. At stages 2 and 3, as the saturation deficit decreases, that is, as it gets wetter, there is an exponential increase in the release of N.

streams) will have low soil saturation deficits, while positions with smaller contributing drainage areas and higher surface slopes (i.e., near ridges) will have high soil saturation deficits. These localized differences in soil saturation deficits can cause significant variations in canopy biogeochemical cycling rates within the hillslope [*Band*, 1993; *Band et al*., 1993]. To account for catenary controls on the local soil saturation deficits, we compute a catenary index (CI) that is based on the assumption of a steady state subsurface throughflow system in which recharge from the unsaturated to the saturated zone in the contributing area above a unit length of contour is equal to the saturated throughflow across the contour length [*Beven*, 1986]:

$$CI = \ln\left[\frac{aT_e}{T_i \tan \beta}\right] \tag{4}$$

CI catenary index, dimensionless.
a contributing area, m^2.
T_i local soil transmissivity, m d^{-1}.
$\ln [T_e]$ areal average of $\ln [T_i]$, $[1/a \int \ln [T_i]\, da]$, m d^{-1}.
β local gradient, deg.

The catenary index is used to compute local saturation deficits S_i:

$$S_i = S_h + m(\lambda - CI) \tag{5}$$

S_i is the local soil saturation deficit in meters; m is a parameter proportional to the rate of change of saturated hydraulic conductivity with depth; and λ is hillslope mean catenary index ($\int \ln [aT_e/T_i \tan \beta]\, da$). A frequency distribution of the catenary index is computed for each hillslope.

For each interval of the frequency distribution, interval-specific simulation of biogeochemical processes enables simulation of the nonlinear impacts and interactions of drier and wetter parts of the hillslope on biogeochemical processes. At the end of each time step the interval-specific fluxes are area-weighted to update the hillslope-specific fluxes, and the hillslope-specific soil saturation deficits are area-weighted to update the catchment-specific soil saturation deficit S, which forms the basis of the N flushing mechanism.

2.4. The N Flushing Hypothesis

Following *Hornberger et al*. [1994], catchment flushing behavior is characterized by peak concentrations of N occurring prior to peak water discharge, with continuously and rapidly declining concentrations as the melt or rain event proceeds. *Hornberger et al*. [1994] argued that, whereas mixing of waters from a temporally constant-concentration reservoir with melt or rain water represents a dilution response with a hyperbolic relationship between concentration and discharge, the mixing of waters from a temporally variable-concentration reservoir with melt or rain water represents a flushing response with a complex relationship between concentration and discharge. For N, assessing this temporal variability involves the added complexity of anticipating the catchment's biological demand for N. The catchment fluctuates between being a potential sink and a potential source of N. We use the terms sink and source relative to the receiving stream: sinks retain N that drains into them, whereas sources release N back either to the air (as NO, N_2O) or to downslope areas and adjacent waters (as NO_3^-, NH_4^+, or dissolved organic nitrogen, although NO_3^- is the most mobile form of nitrogen). The N flushing hypothesis considers that when the catchment is a potential source of N the release of N to adjacent waters varies as a function of the soil saturation deficit (Figure 3). The specific hydrological controls on the flushing of N are hypothesized to include (1) the catchment-average soil saturation deficit, (2) its rising and recessional oscillations; (3) its frequency; and (4) its covariance with the concentration of N in the soil. The extent of accumulation of N in the soil is a function of the properties of the soil (including temporally variable soil temperature and moisture and their controls on the rates of microbial-based transformations of nitrogen from immobile to mobile forms), following an exponential decline moving from the highly bioactive soil surface down the soil profile. When the soil saturation deficit S is high, the low water table allows for the accumulation of N in the soil profile resulting in low release of N into adjacent waters. As S declines, the rising water table flushes water-soluble N from the soil profile. When $S = 0$, the soil profile is saturated and N formed in the high bioactivity zone of the soil surface is released resulting in high release of N into adjacent waters.

3. Test Area

The Turkey Lakes Watershed (TLW) (10.5 km^2) is an old-growth sugar maple forest on the Canadian Shield in the Algoma Highlands of central Ontario, Canada (Figure 4). The TLW contains a chain of lakes fed by small headwater catchments that ultimately drains into Batchawana Bay on the eastern shoreline of Lake Superior.

The TLW represents a reasonably undisturbed region. The landscape receives a moderate level of atmospheric deposition—annual values of total (wet plus dry) deposition ranged from 34 to 38 (±15%) mmol m^{-2} yr^{-1} for sulphate and 38 to 47 (±30%) mmol m^{-2} yr^{-1} for nitrate [*Sirois and Vet*, 1988].

The closest point source emitters of air pollutants are the steel mill coke ovens located 60 km south in Sault Sainte Marie, Ontario, and an iron ore sintering plant located 100 km north in Wawa, Ontario. The influence of both of these point sources is minimized by the predominantly westerly wind direction [*Jeffries and Semkin*, 1982].

The TLW climate is continental, strongly influenced by the proximity of Lake Superior. The TLW topography is controlled by the bedrock with 400 m of relief from its outlet (at 244 m above sea level (asl) to the predominant summit of Batchawana Mountain (at 644 m asl)). A set of major faults cut through the bedrock and control the drainage patterns [*Jeffries and Semkin*, 1982]. The bedrock is composed of generally insoluble, mafic metavolcanic rock ranging from andesite to basalt, with granite present near the summit of Batchawana Mountain [*Giblin and Leahy*, 1977]. The bedrock is overlain by a thin and discontinuous till. The thickness of the till varies from <1 m at higher elevation locations (with infrequent surface exposure of bedrock) to 1–2 m at lower elevations [*Jeffries and Semkin*, 1982]. There is an occasional occurrence of deep till deposits (up to 65 m) in local bedrock depressions and/or along bedrock fault lines [*Elliot*, 1985]. The till consists of two layers: an upper ablation till which is a silty to sandy till and is relatively permeable (10^{-3} cm s^{-1} saturated hydraulic conductivity), and a lower basal till which is a compact sandy till and is relatively impermeable (10^{-5} cm s^{-1} saturated hydraulic conductivity) [*Nicolson*, 1988]. At low to moderate elevations the ablation till overlies the basal till at a depth of about 0.5 m. At high elevations the basal till is intermittent and the ablation till overlies bedrock. The soils that have developed in the tills are Orthic Ferro-Humic and Humo-Ferric podzols. Dispersed pockets of highly humified organic deposits (Ferric Humisols) are found at all elevations in bedrock-controlled depressions and adjacent to lakes and streams [*Canada Soil Survey Committee*, 1978; *Cowell and Wickware*, 1983]. The sugar maple trees are generally shorter and of poorer quality at higher elevations (>460 m asl), indicating a combination of climatic and nutrient stresses at some topographic positions within the landscape [*Nicolson*, 1988].

Nested within the TLW, catchment 31 (C31) is a small, first-order stream that drains an upland of 4.64 ha on the northeastern side of the main stream (Figure 4). Catchment 31 was selected to test the N flushing hypothesis. Catchment 31 is characterized by two dominant hillslopes (south facing and west facing aspects) with an average slope of 12°, and a range of elevation from 365 m at the weir to 440 m at the ridgeline. Catchment 31 typically experiences two seasonal hydrographs: the first during spring snowmelt and the second during autumn stormflow, as precipitation increases and evapotranspiration decreases.

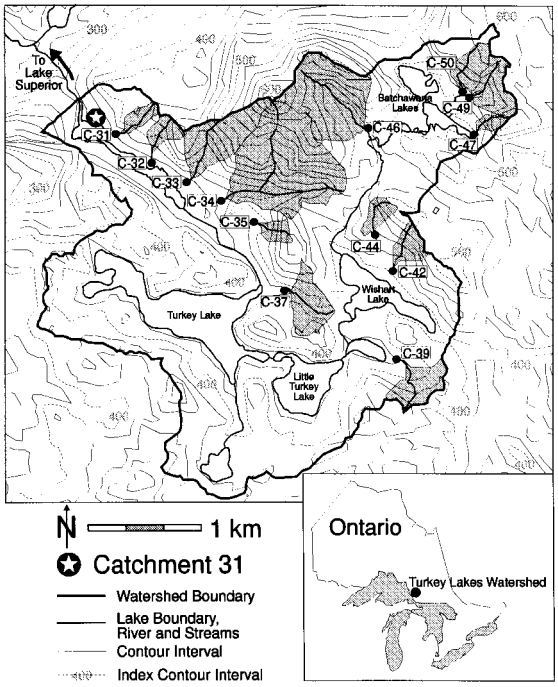

Figure 4. Location of the Turkey Lakes Watershed (centered at 47°03′00″N and 84°25′00″W). The analyses presented in this paper focuses on catchment 31 (C31), a 4.64-ha headwater catchment in the northeastern portion of the watershed.

4. Methods

4.1. TLW Simulation Model

The TLW landscape was partitioned into hillslopes, ridge lines and streamlines, organized around the TLW drainage network according to the methods of *Band* [1989], *Lammers and Band* [1990], and *Mackay and Band* [1994]. Once delimited, each hillslope was parameterized for canopy, topographic, and soil information. Canopy lifeform was composed of about 90% sugar maple (*Acer saccharum* Marsh.), 7% yellow birch (*Betula alleghaniensis* Britton), and other minor species. Since the canopy was dominated by sugar maple, the canopy lifeform was assumed to be constant over space. Canopy leaf area index (LAI) data was derived from Landsat TM data [*Nemani et al*., 1993] that was calibrated using a combination of DECAGON Sunfleck Ceptometer-derived LAI data and allometrically derived LAI data. Topographic attributes (i.e., slope, aspect, elevation, contributing area) were derived from digital terrain analysis [*Evans*, 1980; *Band*, 1986, 1989]. Soil attributes, including effective mineral soil depth, were derived from field and literature surveys. On the basis of these surveys a polynomial equation was derived to distribute the effective mineral soil depth as a function of the catenary position. Other soil properties, including saturated hydraulic conductivity and the rate of change of saturated hydraulic conductivity with soil depth, were more difficult to derive, and therefore these Topmodel parameters were optimized for catchment 31 using the SIMPLEX optimization routines of *Press et al*. [1988] and confirmed with the limited data that were available.

Daily precipitation and temperature data were collected at an Atmospheric Environment Service (AES) meteorological recording station located at the southeast boundary of the TLW. Missing data were estimated by linear regression based on data from the closest meteorological stations within the area for which complete records were available (Montreal Falls and Sault Sainte Marie, Ontario). *Semkin and Jeffries* [1986] cited a significant spatial variation in precipitation within the TLW due to orographic effects. On an annual basis, there was an average of 10% smaller water-equivalent snowpack at catchment 31 compared to the AES meteorological recording station. The snow precipitation for all years at catchment 31 were therefore adjusted downward by 10%.

The TLW site and physiological constants were derived from field and literature data (Table 1).

Table 1. RHESSys Parameters for Turkey Lakes Watershed (Included in Site.ini and Biome.ini Initialization Files)

Parameter	Parameter Description	Source
	Site Initialization File	
variable	effective mineral soil depth, m	field data, *Jeffries and Semkin* [1982]
0.2	effective mineral soil porosity (porosity-field capacity), m	field data, *Dunne and Leopold* [1978]
2.25	saturated hydraulic conductivity, K_0, m d^{-1}	field data, *Nicolson* [1988]
0.08	extinction of Ko with depth, m	field data, *Nicolson* [1988]
−5.0	snowpack energy deficit, °C	modified for TLW, after *Running and Coughlan* [1988]
0.0022	temperature melt coefficient	modified for TLW, after *Running and Coughlan* [1988]
0.14	radiation melt coefficient	modified for TLW, after *Running and Coughlan* [1988]
	Biome Initialization File	
6.0	canopy closure LAI	field data
70.9	specific leaf area, m^2 kg C^{-1}	*Morrison et al*. [1993]
135	leaf on date (yearday), incremented over 7 days	field data
259	leaf off date (yearday), decremented over 28 days	field data
0.0005	canopy precipitation interception coefficient, m LAI^{-1}	*Running and Coughlan* [1988]
0.02	litter precipitation interception coefficient, m	*Running and Coughlan* [1988]
−0.5	light extinction coefficient, LAI^{-1}	*Running and Coughlan* [1988]
0.0045	maximum stomatal conductance, m s^{-1}	*Running and Hunt* [1993] *Kelliher et al*. [1995]
0.0008	maximum mesophyll conductance, m s^{-1}	*Running and Coughlan* [1988]
0.3	aerodynamic conductance, m s^{-1}	modified for TLW, after *Running and Coughlan* [1988]
−2.0	critical leaf water potential, MPa	*Running and Coughlan* [1988]
	maximum photosynthetic rate, μmol m^{-2} s^{-1}	*Running and Hunt* [1993]
0.4	leaf maintenance respiration, kg C kg d^{-1}	*Running and Hunt* [1993]
0.2	stem maintenance respiration, kg C kg d^{-1}	*Running and Hunt* [1993]
0.2	root maintenance respiration, kg C kg d^{-1}	modified for TLW, after *Running and Hunt* [1993]
0.0216	leaf N concentration, kg N ha^{-1}	*Morrison* [1985]
1.0	leaf (kg C ha^{-1}): leaf (kg C ha^{-1})	*Morrison et al*. [1993]
51.7	stem (kg C ha^{-1}): leaf (kg C ha^{-1})	*Morrison et al*. [1993]
8.9	root (kg C ha^{-1}): leaf (kg C ha^{-1})	*Morrison et al*. [1993]
2.2	LAI to projected LAI	field data

4.2. Nitrate-N Release

Total daily water discharge (meters per day) was derived from a continuously measured stream gauge station equipped with a 120° V-notch weir on catchment 31 (correlation between discharge and stage height was within the ±5% error range). Missing data (usually winter low flow) were estimated by linear regression with an adjacent catchment for which there was a complete record (for catchment 31, on an annual basis, <3% of daily discharge data were missing). Nitrate-N concentrations (milligrams per liter) in the water discharge were derived from stream water samples collected every 2 weeks during the winter, daily during spring snowmelt, and weekly or every 2 weeks during the summer and autumn [*Nicolson*, 1988]. Samples were collected at the same sampling point, in the center of the stream, during each visit. To remove particulate matter, each sample was filtered through a Whatman no. 41 filter that had been rinsed with distilled water. For each sample a 100-mL subsample was filtered through a 0.45-μm filter that had been washed with distilled water and stored without preservative at 5°C in a bottle that had been washed with acid (0.1N H_2SO_4) and rinsed with distilled water. The 100-mL sample was analyzed for NO_3^--N within 1 week of collection by cadmium reduction using a Technicon AutoAnalyzer II-C+. N flux (kg m^{-2} d^{-1}) was derived by the product of the daily water discharge (meters per day) and the N concentration in the discharge (milligrams per liter) for a day for which both nutrients and water were analyzed [*Nicolson*, 1988].

At a minimum an ideal data set would include discharge and the concentration of N in discharge for each day of the study period. Unfortunately, the data were limited to the previously described sampling protocol. This limitation posed no problems in our analyses, as (1) we restricted our analyses to days for which both discharge and N in discharge data were available, and (2) we simulated the catchment soil water saturation deficit conditions surrounding the days for which data were available. However, this limitation resulted in a greater num-

ber of data representing the spring snowmelt period compared to the other seasons, and therefore the full range of the flushing conditions were not represented equally.

4.3. N Flushing Index

The flushing status was modeled as S, the catchment-average saturation deficit, and S/S_x, the ratio of the catchment-average saturation deficit to the previous x-day average saturation deficit. While S considers only the current day saturation deficit, S/S_x incorporates S, the rising and recessional limbs of S, and to some degree the frequency of the oscillations in S by considering the ratio of S to the average saturation deficit over the previous x time period. The S/S_x index can be segregated into three distinct scenarios:

1. If $S/S_x < 1$: The current day water table is higher than before and saturated throughflow is rising into previously unsaturated parts of the soil profile (i.e., catchment is flushing).
2. If $S/S_x > 1$: The current day water table is lower than before and saturated throughflow is receding (i.e., catchment is draining).
3. If $S/S_x = 1$: There is no change in the water table relative to the previous x-day period.

For S/S_x, several periods of time (x) were considered to determine the optimal length of time between consecutive flushings to permit accumulation of N in the soil profile [*Creed et al*., 1994]. Clearly, the optimal length of time is a function of the season, with longer periods of time required in the winter than in the summer.

For general analyses, we selected a constant length of 30 days (i.e., S/S_{30}). This selected length is suitable for the longer timescale (or broader base) of the oscillations related to the dominant spring flushing but may be too long for the shorter timescale (or narrower base) of the oscillations of the late summer and early autumn flushings. For example, during a dry summer in which a long dry period is followed by a short wet period, the recessional limb of the soil saturation deficit of the hydrological event may be incorrectly identified as flushing when it should be draining (i.e., $S/S_{30} < 1$ but S_{30} is dominating the response). When necessary, for specific analyses, we selected a constant length of 3 days (i.e., the daily derivative of S, where positive values indicate the rising, flushing limb and negative values indicate the recessional, draining limb of the oscillation) and 1 day (i.e., S) to resolve the characteristics of the shorter timescale of the oscillations of the late summer and early autumn flushings.

The flushing indices infer that, if high concentrations of N in the stream occur only during the flushing process, the release of N occurs by a mechanism regulated by a saturated throughflow process that is either coupled to the groundwater system (e.g., rising water table) or not coupled to the groundwater system (e.g., rising perched water table). It should be emphasized that since S represents the average of the distribution of soil saturation deficits within the catchment, the rising saturated throughflow system can occur either at the catchment-scale, when S is low, or at the subcatchment-scale, when S is high but one tail of the distribution of soil saturation deficits is low. In contrast, if high concentrations of N persist during the subsequent draining process, the release of N occurs by a mechanism other than a saturated throughflow process.

4.4. N Source Index

The discrimination of a catchment as a potential sink area (demand > supply) or source area (supply > demand) of N is a complex and current research area. A simple approximation of a catchment's N sink versus source strength was computed as follows. We assumed that C cycling activity was stoichiometrically related to N cycling activity, and therefore the C source index was used as a N source index. This assumption could only be manifested in soils with high nitrification rates, where there is a 1:1 transformation of organic-N to inorganic NO_3^--N, such as those found at the TLW [*Foster*, 1989]. A relative C source index (equation (6)) was modeled as the ratio of C supply to C demand (equation (7)). C supply was modeled as gross macromolecular C decomposition, an exponential function of the maximum rate of macromolecular C decomposition modified by moisture and temperature factors (after *Parton et al*. [1987], with coefficients based on a deciduous, temperate forest). A weakness of the C supply computation was that we computed gross and not net C supply, as we did not consider the role of the microbial community on the C transformation process. C demand was modeled as net canopy C fixation.

$$\text{relative source index} = \text{source}/\text{source}_{\max} \tag{6}$$

source is the nutrient availability index, dimensionless; and $\text{source}_{\max}$ is the maximum nutrient availability index, dimensionless.

$$\text{source} = \frac{\text{supply}}{\text{demand}} = \frac{(1 - e^{-\text{MF}\cdot\text{TF}})}{\text{PSN} - \text{RESP}} \tag{7}$$

MF moisture factor (scaled to 0–1).
TF temperature factor (scaled to 0–1).
PSN canopy photosynthesis, kg C m^{-2} d^{-1}.
RESP canopy respiration, kg C m^{-2} d^{-1}.

Although soil temperature and moisture influence the mineralization of N, the C:N ratio of the soil has an overriding influence. C:N determines the fate of mineralized NH_4^+-N (i.e., net N immobilization versus net N mobilization). A C:N = 20 has been considered to be the threshold for determining net N immobilization (C:N > 20) or net N mobilization (C:N ≤ 20) [*Alexander*, 1977; *Van Miegroet et al*., 1992]; however, the critical C:N threshold value may vary with climate [*Berg and Staaf*, 1981]. Considerable NO_3^--N formation in acid, hardwood soils has been reported throughout the northeastern United States and Canada [*Krause*, 1982; *Mollitor and Raynal*, 1982; *Federer*, 1983; *Klein et al*., 1983; *Foster*, 1985, 1989]. In sugar maple podzols the forest-floor layers are the location of the most intense microbial activity and therefore the location of the most N release [*Parkinson and Coups*, 1963]. In the TLW forest-floor layers the relatively low and narrow range of C:N ratios (e.g., L layer, C:N = 25–29; F layer, C:N = 21–24; H layer, C:N = 22–24, based on 6 sites) favors high nitrification rates. For example, *Foster* [1985, 1989] observed that in the TLW forest-floor layers, nitrification rates equalled mineralization rates, while the NH_4^+-N pool remained small. Prior to application to other sites, however, a N source index including other important factors regulating both nitrification (e.g., C:N) and denitrification would have to be developed.

5. Results and Discussion

5.1. General Description of the Study Period (1981–1990)

The 10-year period from 1981 to 1990 forms the basis of this study. Included in this decade were extremes in the 50-year climatic record, including two years of severe summer droughts

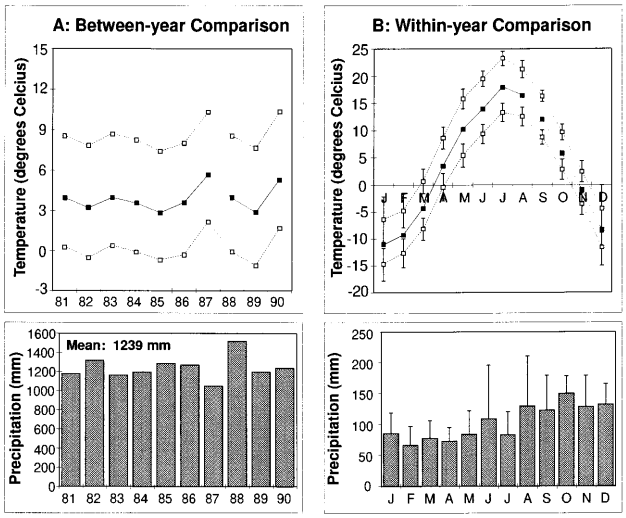

Figure 5. Temperature and precipitation patterns at the Turkey Lakes Watershed: (a) between-year comparison of average, maximum, and minimum annual temperature and total annual precipitation; and (b) within-year comparison of average, maximum, and minimum monthly temperature (±1 standard deviation) and total monthly precipitation (±1 standard deviation).

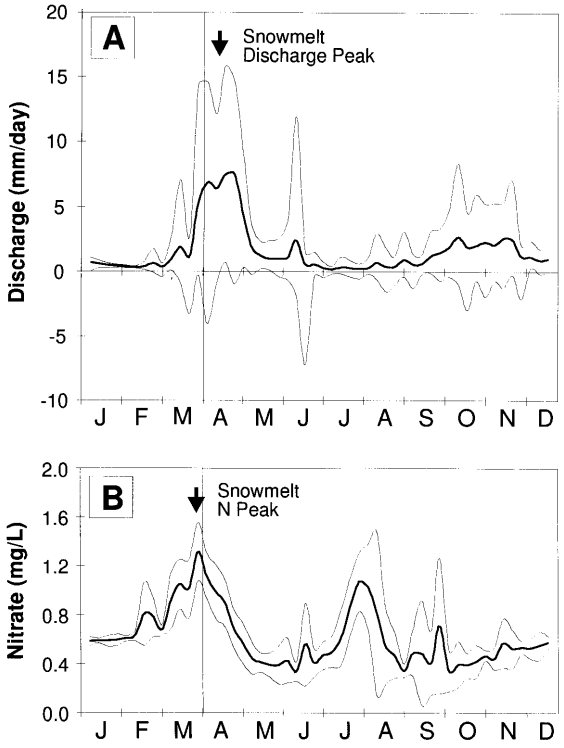

Figure 6. Temporal patterns of discharge and the concentration of NO_3^--N in discharge: (a) average weekly discharge (10-year average ± 1 standard deviation); and (b) average weekly concentration of NO_3^--N in discharge (10-year average ± 1 standard deviation). The line included in each graph is to facilitate comparison of the timing of the snowmelt peaks in discharge and NO_3^--N in discharge, the discharge peak occurring approximately 2 weeks after the NO_3^--N peak.

(1982–1983 and 1988–1989). The mean annual temperature and precipitation averaged 3.9°C (range: 2.8°–5.7°C) and 1239 mm (range: 1047–1515 mm), respectively (Figure 5a). Within-year variations in seasonal precipitation were greater than between-year variations in annual precipitation. Seasonal patterns in precipitation show peak precipitation in the autumn with lower but uniform precipitation in the winter and spring and variable precipitation in the summer (Figure 5b).

Catchment flushing behaviour was observed (Figure 6). Discharge is presented in Figure 6a and the release of N in discharge is presented in Figure 6b. With a baseline concentration of N of approximately 0.5 mg L^{-1}, peak concentrations of N occurred just prior to the spring high flow and in late summer low flows. In spring a primary peak in the concentrations occurred about two weeks prior to peak water discharge, with declining concentrations as the spring snowmelt proceeded, indicating an exhaustion of the N reservoir over prolonged saturated conditions. In summer a secondary peak in the concentrations occasionally occurred (Figure 6b). While the concentrations (milligrams per liter) of N were high in both winter and summer, the fluxes (kg ha^{-1} d^{-1}) of N were high only in late winter to early spring during the dominant snowmelt discharge period. No significant relationship was observed between discharge and the concentration of N (Figure 7). The concentration of N was influenced by the intensity and frequency of hydrological events. After several storms the concentration of N would show a negligible response to discharge, reflecting the insufficient time for reaccumulation of N in the reservoirs of N within the catchment. As expected, a significant relationship was observed between discharge and the mass of N, with the mass of N increasing as a linear function of discharge in all seasons (i.e., N in discharge (kg ha^{-1} d^{-1}) = 2.17 × discharge (mm d^{-1}), $r^2 = 0.92$).

5.2. RHESSys Simulation Results

5.2.1. Model validation. RHESSys validation was performed on available simulated and observed discharge data. RHESSys provided reasonable simulations of the discharge hydrographs (i.e., simulated discharge = 0.95 × observed discharge, $r^2 = 0.64$). In comparing the observed and simulated discharge, high and low flows matched with no significant time lag. Over the 10-year period the difference between simulated and observed totals are close to 0%; for any given year the difference ranged from −15% to +15%. There was one exception (1989) where frequent short summer rainstorms at the AES meteorological station that were not experienced at catchment 31 resulted in simulated discharge 30% higher than observed discharge. Although the absolute value of the high flows were reasonably matched, the absolute value of the low

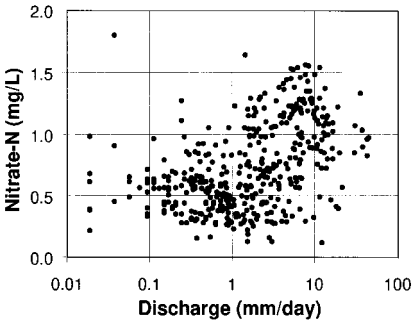

Figure 7. Relationship between discharge and the concentration of NO_3^--N in discharge.

flows tended to be overpredicted. It was difficult to know if the lack of fit as we approached the lower limit of the discharge distribution (0.05 mm d^{-1}) was a problem of overprediction by simulated data or underprediction by observed data. On the basis of field observations, the observed data may have underpredicted low flows because of the measurement limitations of the 120° V-notch weir and/or because of loss of drainage water via percolation through the fractured bedrock that is characteristic of the catchment area.

5.2.2. Hydrological processes. The simulated soil saturation deficits underwent seasonal oscillations during the year, with oscillatory maxima in winter and summer (Figure 8). For all 10 years the snowmelt period was at or near saturation ($S = 0$). During other periods of the year, the soil saturation deficits were variable. In winter, soil saturation deficits were largely controlled by the wetness of the previous autumn. If there was high precipitation during the previous autumn, the soils remained near saturation during the winter. In contrast, if there was low precipitation during the previous autumn, the soils remained drier during the winter. In summer all years experienced a significant increase in saturation deficits, with the primary difference between a wet and dry year being the amplitude of the summer oscillation.

On the basis of the simulated hydrological partitions, on average, approximately 33% of the cumulative annual discharge was routed through the surface, and 67% was routed through the subsurface flow partitions. The dominance of the subsurface flow partitions is of particular importance to the flushing hypothesis. Among the 10 years the proportion of base flow was uniform (range: 162–217 mm total annual baseflow), while return flow (caused by seepage from saturated areas) and surface flow (caused by direct precipitation onto saturated areas) were variable, with a smaller proportion of these flows in dry years (e.g., in 1987, 48 and 173 mm for return and surface flows, respectively) compared to wet years (e.g., in 1988, 277 and 347 mm for return and surface flows, respectively) (Figure 9). Return flow occurred primarily during snowmelt with an occasional occurrence in years characterized by substantial autumn stormflow (Figure 10). Surface flow occurred during most runoff-generating events, indicating that portions of the catchment remained saturated or nearly saturated during both dry and wet years (Figure 10). No significant relationships were found between the different simulated partitions of discharge hydrograph and the release of N (similar to Figure 7). Therefore neither daily total discharge or daily par-

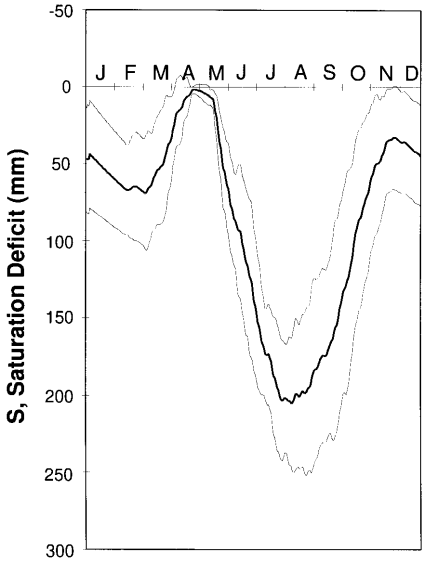

Figure 8. Temporal pattern of daily saturation deficit S (10-year average ± 1 standard deviation). When $S = 0$, the water table is at the soil surface, and, as S increases, the depth of the water table increases.

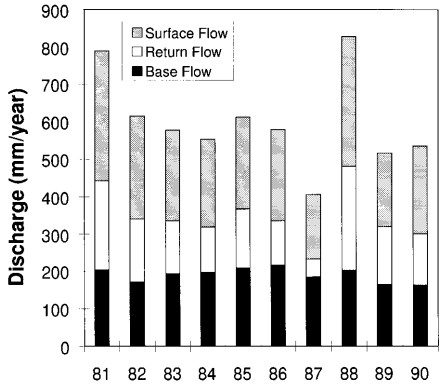

Figure 9. Between-year comparison of the hydrological flow partitions, including surface flow, return flow, and base flow partitions.

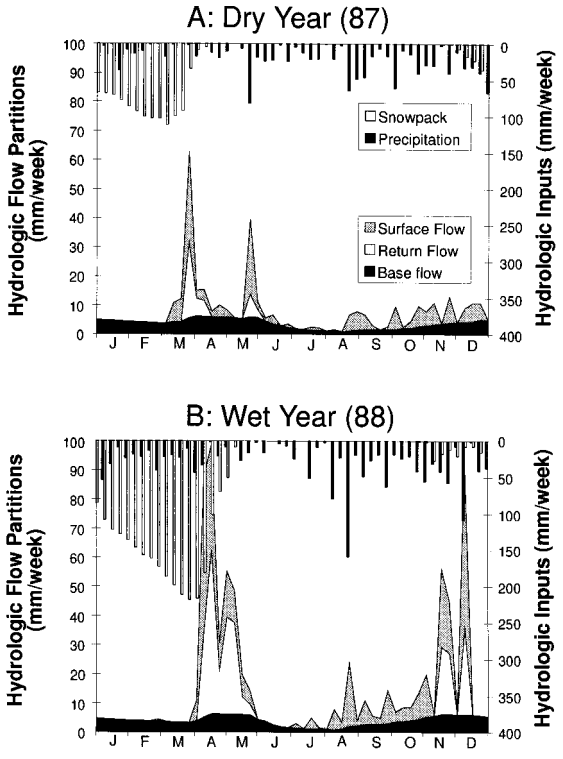

Figure 10. Within-year comparison of hydrological flow partitions: (a) a relatively dry year (1987), with spring snowmelt dominating the annual hydrograph; and (b) a relatively wet year (1988), with spring snowmelt and autumn stormflow dominating the annual hydrograph. The hydrological flow partitions (based on left-hand axis) and the hydrological inputs (based on right-hand axis) represent weekly totals.

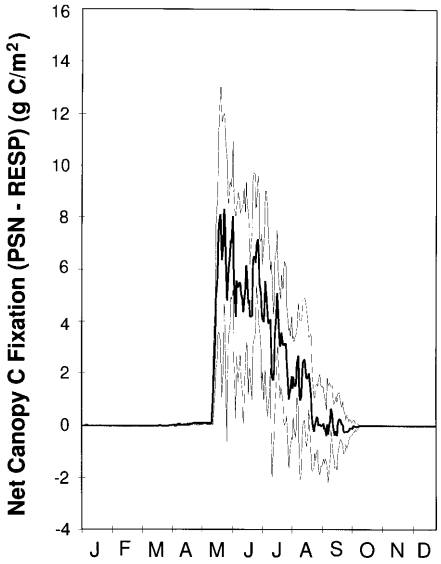

Figure 11. Temporal pattern of daily net canopy carbon fixation, PSN − RESP (10-year average ± 1 standard deviation).

titioned discharge from the catchment provided a predictive tool for the concentration of N in discharge waters.

5.2.3. Physiological processes. As an old-growth forest, the forest on catchment 31 has a relatively stable biomass. Between-year patterns in net C fixation rates showed a slight net gain in annual biomass over 1980–1985 and a slight net loss in annual biomass in 1986–1990. Within-year patterns in net C fixation rates were as follows: slightly negative rates during the nonfoliage period, high rates (on average, 8 g C m^{-2}) during the late spring to early summer period, moderate rates (4–8 g C m^{-2}) that were maintained up to the midsummer period, and then low rates that declined steadily from midsummer through the remainder of the foliage period (Figure 11). The decline in net C fixation rates in the later foliage period may have reflected an increasing limitation to forest growth by water. Soil saturation deficits were high in the summer (Figure 10). The forest responded to the high soil saturation deficits with decreased rates of PSN but maintained rates of RESP which resulted in net C fixation rates reaching a C deficit in some years. This decline in the net C fixation rates had important implications for catchment N dynamics as the catchment would have become a source of N to the stream at least for some portions of the year.

5.3. N Flushing Index Versus N Release in Discharge Waters

The flushing mechanism (Figure 3) as modeled by the soil saturation deficit S was not observed in the relationship between S and the concentration of N in discharge waters (Figure 12). Rather, the relationship showed an envelope response and, although the outer limit of the envelope showed the anticipated decline in N with increase in S to a soil saturation deficit of about 200 mm, an unanticipated increase in N with increasing S was observed at soil saturation deficits greater than 200 mm. Possible processes controlling the release of N were investigated by examining the relationship between S and the release of N over individual years (Figure 13). In winter, low to moderate S co-occurred with high-N release from the catchment, emphasizing the importance of the contributions of the winter period to the release of N. During the wet periods of the year, in spring and autumn, the expected co-occurrence of low-S and high-N release was observed. In the spring snowmelt period there was a primary peak of N release and, during years where there was an autumn stormflow period, there was a secondary peak of N release. The difference in primary and secondary peaks in the single-year analysis contributed to the envelope response depicted in the composite-year analysis (Figure 12). In late summer and/or early autumn, when S dropped below 200 mm, there was an unexpected co-occurrence of high-S and high-N release.

The flushing mechanism as modeled by S/S_{30} was depicted in the outer limit of the envelope response of the relationship between S/S_{30} and the release of N in discharge waters (Figure 14). During draining states ($S/S_{30} > 1$) there was a narrow range in the concentrations of released N, representing baseline concentrations. During flushing states ($S/S_{30} < 1$) there was a broad range in the concentrations of released N.

Further examination of the hydrological conditions during the release of high concentrations of N revealed two distinct populations: a low-S and a high-S population (the release of high concentrations of N never occurred with the intermediate-S population) (Figure 15a). The low-S population was flushing ($S/S_{30} < 1$). The high-S population showed a very narrow range in S/S_{30} (~1.0). To determine if the high-S population was flushing or draining, we examined the relationship between the release of N and the daily derivative of S (Figure 16) and S (Figure 17). Through these analyses we found that the high-S population represented a combination of both flushing and draining states (Figure 16), however, during severe summer droughts, in 1982–1983 and 1988–1989, the release of the peak concentrations of N occurred during a flushing state (Figure 17). Since the high-S population represented a combination of both flushing and draining states, we concluded that there must be two mechanisms for the release of N, a rapid flushing, when S is low or high, and a slow draining mechanism.

When $S = 0$, in spring and autumn, the release of N is

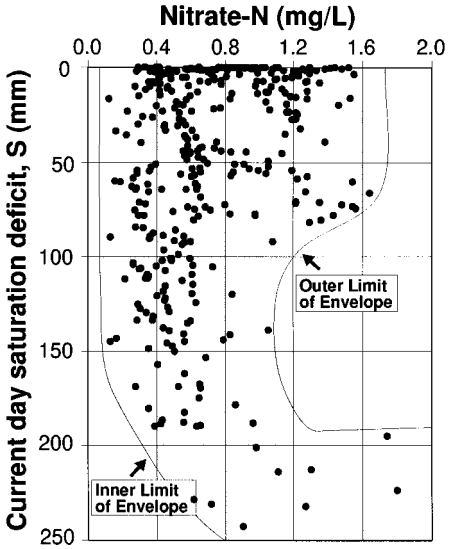

Figure 12. A 10-year composite analysis of the observed concentration of NO_3^--N in discharge as a function of the simulated catchment flushing index S. The shaded area represents the envelope response with the inner and outer limits of the envelope identified.

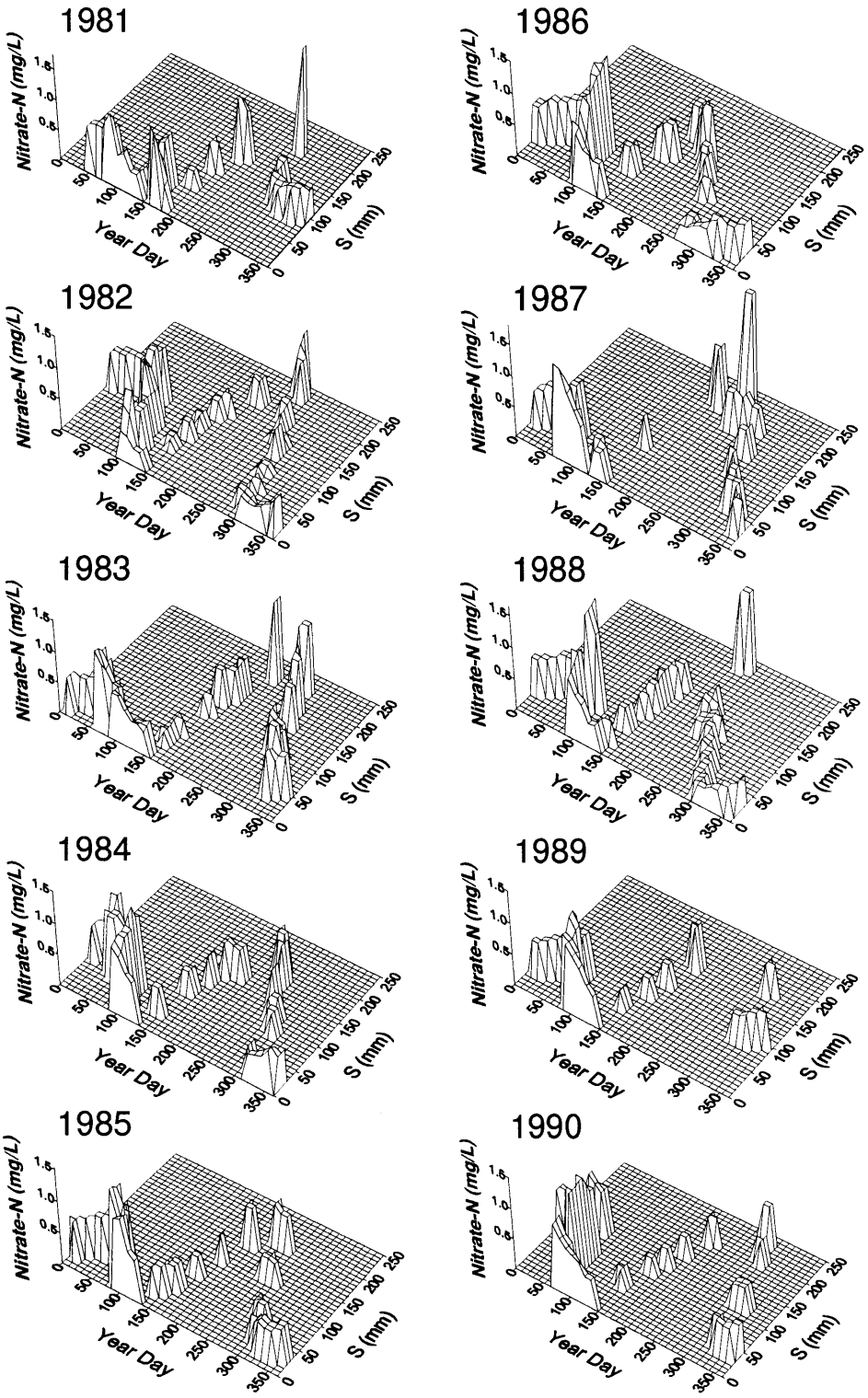

Figure 13. Individual year analysis of the observed concentration of NO_3^--N in discharge as a function of the simulated catchment flushing index S. In this three-dimensional representation, flat areas represent "no data" and not "0 mg L^{-1}."

regulated by a catchment-scale flushing of the N-enriched forest soil layers by saturated throughflow. In the TLW, evidence of significant saturated throughflow is provided by *Bottomley et al*. [1984, 1986], who used isotope techniques to show that, during major hydrological events, event water infiltrates the shallow till deposits, raises the water table, and displaces preevent water that is stored in the soil to the stream. For example, during spring snowmelt and autumn stormflow, water infiltrates the shallow till deposits (<1 m) and moves through the N-enriched forest organic and mineral soil layers and lat-

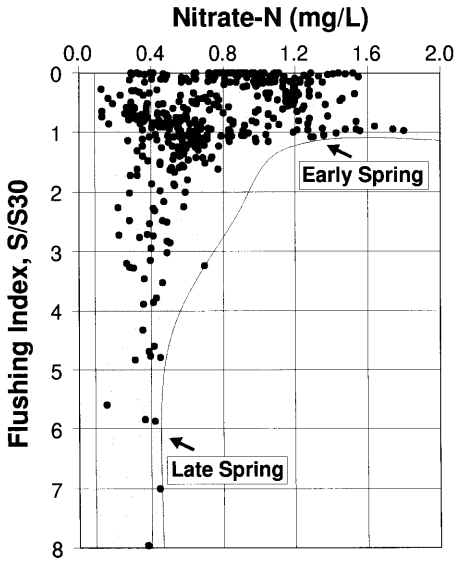

Figure 14. A 10-year composite analysis of the observed concentration of NO_3^--N in discharge as a function of the simulated catchment flushing index S/S_{30}. The shaded area represents the envelope response. The outer limit of the envelope response is dominated by data collected from early spring in the flushing state ($S/S_{30} < 1$) and by data collected from late spring in the draining state ($S/S_{30} > 1$).

erally along the basal till-bedrock interface or, more commonly, along the ablation-basal till interface due to the formation of a perched water table, providing a rapid supply of water downslope [*Bottomley et al*., 1984, 1986; *Nicolson*, 1988]. The rise in the level of saturated throughflow then flushes the N from the soil to the stream.

Other field-based studies provide support for a rapid flushing by saturated throughflow. During hydrological events, *Anderson and Burt* [1982] observed a rapid growth of the catchment's saturated zone, as infiltrating water was rapidly transmitted down to the saturated zone, deepening and enlarging the zone, causing an increase in the discharge of saturated throughflow to the stream. The rapid transmission of water to the water table could arise from several processes: (1) matrix flow, as the relatively high hydraulic conductivity of the surface soil will allow a rapid transport of water to the saturated zone, particularly in areas where the water table is close to the surface (e.g., riparian areas); and (2) macropore flow. Forest soils have extensive macropore systems, including live and dead root channels, and the bouldery nature of the soils [*Tsuboyama et al*., 1994]. *McDonnell* [1990] proposed a "bypass" mechanism to explain the rapid growth of the catchment's saturated zone, where water moves rapidly downward to the bedrock and then laterally over the soil-bedrock interface via macropores. Support for the bypass mechanism was provided by others, including *Tsuboyama et al*. [1994] and *Peters et al*. [1995]. However, *Tsuboyama et al*. [1994] found that although both matrix and macropore flows contributed to the formation of saturated throughflow, matrix flow dominated the discharge (70–93% of total discharge).

In our simulation system we only model matrix flow and, therefore, we may underestimate the timing and the magnitude (depth and extent) of the rising water table.

For the rapid flushing during snowmelt, potential sources of N include the following: (1) the accumulation and formation of N in the snowpack; (2) the preferential elution of this surface N reservoir to the subsurface N reservoir; and (3) the accumulation and formation of N beneath the snowpack in the soil [*Peters and Driscoll*, 1987; *Rascher et al*., 1987; *Shepard et al*., 1990; *Schaefer and Driscoll*, 1993]. During the winter, forest organic and mineral soil layers are substantial sources of subsurface N [*Peters and Driscoll*, 1987]. In the TLW the soils typically remain unfrozen. As long as the soils are not desiccated or saturated, microbial mineralization and nitrification of organically bound N within the soil will occur, albeit at low rates due to the low temperatures [*Foster*, 1989; *Foster et al*., 1989]. If periodic freezing of the soils occurs, the freeze-thaw cycle enhances the shrinking and expansion of N-containing organics resulting in fragmentation of the organic matter and a greater surface area of organic matter for microbial activity [*Wang and Bettany*, 1993, 1994]. Since the supply of N is greater than the demand for N, there is a slow accumulation of N in the soil, and the rate of accumulation increases as the temperature and moisture become more variable prior to the spring snowmelt. The overwinter biotic and abiotic processes, therefore, create a significant source of N in the soil to be flushed in the spring.

For the rapid flushing during stormflow a subsurface N res-

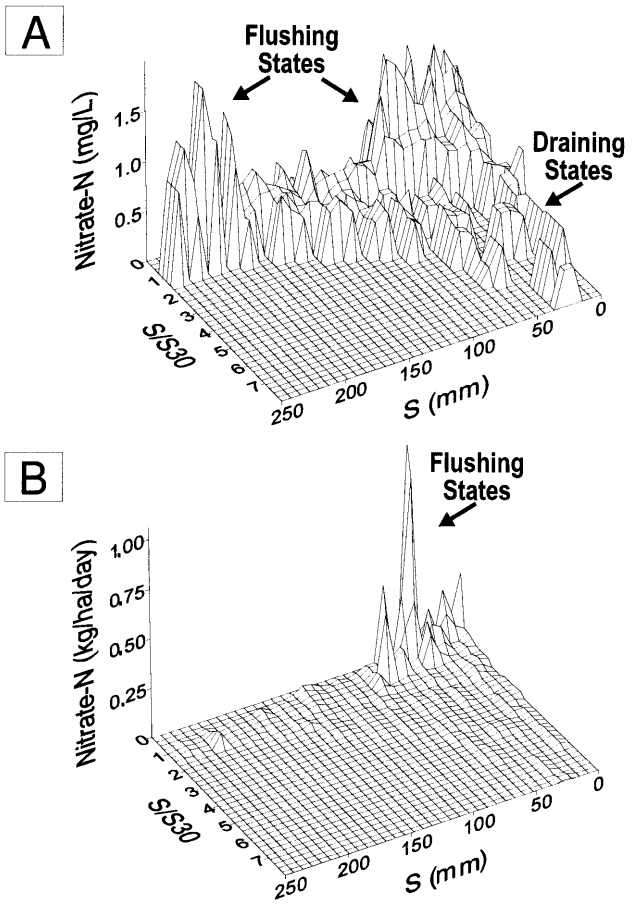

Figure 15. Nitrate-N release as a function of S and S/S_{30}: (a) concentration (mg L^{-1}); and (b) flux (kg ha^{-1} d^{-1}). Flushing occurs both when the water table is high (S = 0 mm) and when the water table is low (S = 250–300 mm). Peak concentrations in the release of N occurs during flushing conditions. Baseline concentrations in the release of N occurs during draining conditions.

ervoir is created as the catchment changes from a net sink to a net source of N. There is a period of time after the net C fixation rates decline and before the canopy leaf fall when under-utilized organic-N and/or NH_4^+-N accumulate in the soil. The immobile organic-N and/or NH_4^+-N create a current source of N (if nitrification rates are not impeded) or a future source of N (if immobile organic-N or NH_4^+-N overwinters and releases mobile N in the spring) that may be flushed [*Foster et al*., 1992]. The implications of the autumn biogeochemical and hydrological dynamics (i.e., flushing versus no flushing of N) are that a dry autumn may result in a high-N flushing spring and a wet autumn may result in a low-N flushing spring, reflecting the inheritability of the characteristics of the dominant spring flushing.

When $S > 0$, the release of N is regulated by a subcatchment-scale flushing by saturated throughflow. As S increases, the catchment becomes a mosaic of hydrological conditions, ranging from dry to wet areas. S represents the average of the distribution of soil saturation deficits. In catchment 31, for example, during the maximum average soil saturation deficit, $S = 300$ mm, local soil saturation deficits ranged from $S_i = 0$ mm (i.e., water table at surface) to $S_i = 500$ mm (i.e., water table below the rooting depth). Previous studies suggest that poorly drained lowland and well-drained upland areas are sinks of immobile NH_4^+-N as the rate of transformation from NH_4^+-N to NO_3^--N is impeded [*Mulholland*, 1992; *Hill and Shackleton*, 1989; *Foster*, 1989; *Foster et al*., 1992]. This study suggests that catchment "hotspots" of flushing activity, such as the transitional area between poorly drained lowland and well-drained upland areas where local soil saturation deficits hover around $S = 0$, may provide a significant source of N to the stream.

Catchment 31 is characterized by considerable expanses of poorly drained lowland areas, the extents of which expand or contract in response to climatic shifts. The periphery of these lowland areas requires only minor oscillations in the water table to create conditions facilitating enhanced nitrification rather than denitrification rates and hence a supply of N that can be flushed. During summer droughts the addition of a small amount of water to the capillary fringe of these areas may result in a rapid and large rise in the water table resulting in large discharges of subsurface water and N to the stream (Figure 17). This subcatchment-scale flushing activity may be driving the release of N, particularly during summer droughts, when catchment-scale flushing activity is at a minimum, and therefore represents an important determinant of low flow water quality.

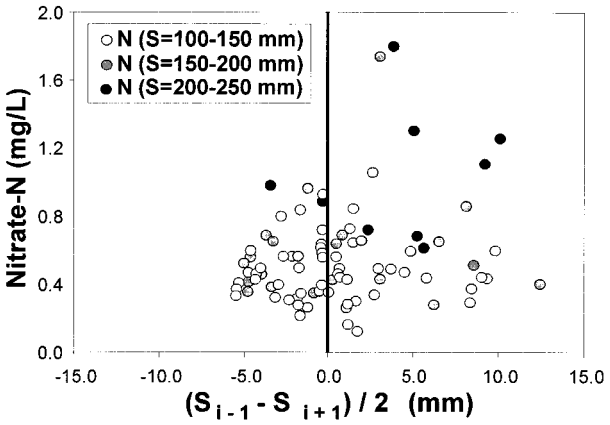

Figure 16. Nitrate-N release as a function of a flushing index based on a 3-day period, $(S_{i-1} - S_{i+1})/2$, where i is the day of year. Plotted data include NO_3^--N concentrations in the stream during periods when the catchment-average saturation deficit is comparatively high, at 100–150 mm (white circle), 150–200 mm (grey circle), and 200–250 mm (black circle). If $(S_{i-1} - S_{i+1})/2 > 0$, catchment is flushing. If $(S_{i-1} - S_{i+1})/2 < 0$, catchment is draining.

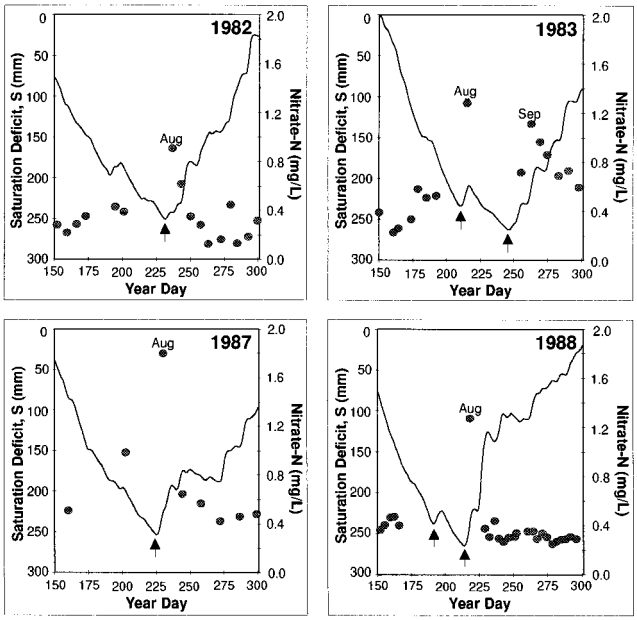

Figure 17. Nitrate-N release as a function of a flushing index based on a 1-day period, S. The graphs depict the concentration of NO_3^--N in discharge during severe summer droughts, in 1982–1983 and 1988–1989, with the timing of the change from draining to flushing states indicated by the inset arrows.

The rapid flushing mechanism therefore occurs during both low-S and high-S states, each state with differential contributions from preevent and event water, as infiltrating water contributes to the formation of a rapidly rising saturated throughflow system.

The slower draining mechanism represents a change in the controlling hydrological flow pathway from a shallow subsurface pathway to a deep subsurface pathway below the rooting depth. We hypothesize that the spring snowmelt or autumn stormflow recharge of deeper waters, either by a slow matrix and/or fast macropore flow, translocates N from the more bioactive upper ablation till into the less bioactive lower basal till. Compared to the ablation till the basal till has a longer residence time and allows for a slower release of N to the stream over the year or over succeeding years. For example, the high concentrations of N observed during late summer low flow may result from the spring translocation of N to deeper subsurface flow paths. This slower draining mechanism indicates that a certain portion of the reservoir of N is isolated from forest uptake by the deeper subsurface flow pathways. In the TLW the hypothesized increase in N in the deeper waters is consistent with the general pattern of increasing N in groundwater from anthropogenic N sources [*Galloway et al*., 1995].

Although a combination of flushing and draining mechanisms appears to result in the observed patterns in the release of N to the stream, during high flows, the low-S flushing state

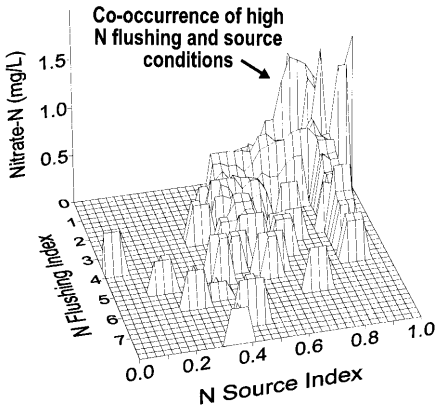

Figure 18. Nitrate-N release as a function of the N flushing index (S/S_{30}) and N source index (scaled to 0 to 1, where 0 is the sink and 1 is the source). Peak concentrations in the release of N are restricted to periods of time when there is a co-occurrence of N flushing and N source conditions, reflecting the combination of hydrological and biogeochemical controls on the release of N from the catchment.

is the dominant mechanism resulting in the high release of N to discharge waters (Figures 15a and 15b), while, during low flows, the high-S flushing state and the draining state are co-dominant mechanisms.

5.4. N Flushing Index Versus N Source Index

While the outer limit of the envelope response of N release as a function of S/S_{30} (Figure 14) can be explained by the N flushing hypothesis, the broad range in N release during flushing states ($S/S_{30} < 1$) suggests that N release is regulated by the size of the variable N reservoir. Plotting N against both S/S_{30} and the source index showed that the release of high concentrations of N required conditions favorable to both flushing and the accumulation of the reservoir of N in the soil (Figure 18). Reduction of either the relative flushing or the relative source of N resulted in significant drops in the concentrations of N in the stream. A temporal analysis of the flushing activity in terms of the catchment's functional state as a N sink (demand > supply) or N source (supply > demand) is provided in Figure 19. On the basis of this analysis, catchment 31 released high concentrations of N to the stream during two periods: just prior to and following the foliage period. Of particular significance is the flushing of N prior to the foliage period which represents a possible decoupling of N routing and N cycling processes as a certain portion of the reservoir of N is flushed from the soil prior to the onset of the forest growing season. The role of the microbial community during this decoupling, in particular, and during the rest of the year requires further study.

5.5. Alternative Explanations

We provide indirect evidence that a variable reservoir of N exists and that this reservoir of N is flushed from the soil to the stream at specific times corresponding to both the rise in the relative level of saturated throughflow in the soil and the relative availability of N in the soil. We do not provide direct evidence of the contributions of N to the stream from the different hydrological sources areas: surface versus subsurface, unsaturated versus saturated, or shallow subsurface versus deep subsurface source areas.

Let us consider two alternative explanations, in which the observed release of N is controlled by (1) surface rather than subsurface processes and (2) unsaturated rather than saturated subsurface processes.

5.5.1. Surface versus subsurface hydrological controls. In the TLW there is a significant reservoir of N in the snowpack [*Semkin and Jeffries*, 1986]. If the concentrations of N are homogeneous within the snowpack, then the peaks of the snowmelt discharge and the concentrations of N in the discharge would coincide as it would be a dilution response. The timing of N peak concentrations during snowmelt (Figure 6) appears to contradict this scenario. If the concentrations of N are heterogeneous in snowpack, for example, N deposited onto the surface of snowpack, and there is a preferential release of this N from the snowpack to the stream, then the peaks of the N discharge would occur prior to the peak of water discharge. In fact, in the TLW, snowmelt studies demonstrate that a preferential release of N from the snowpack to the stream

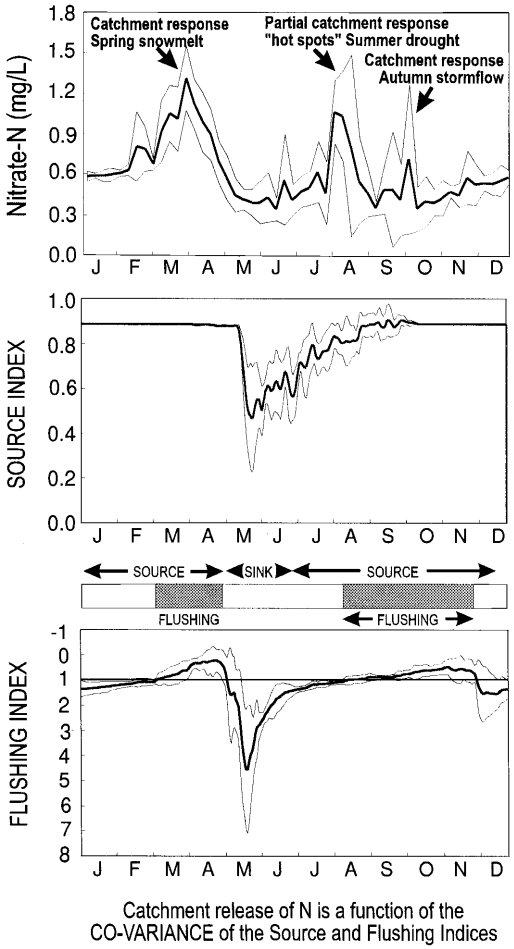

Figure 19. Temporal analysis of the catchment flushing behavior as the catchment fluctuates between a potential source and a potential sink of N to the stream. The time series depict the observed concentration of NO_3^--N in catchment discharge, the simulated N source index and the simulated N flushing index (10-year average $\pm$ 1 standard deviation). The shaded areas between the N source and N flushing time series highlights the periods of the time when there is a co-occurrence of N source and N flushing conditions. These shaded areas correspond to the observed peak concentrations in the release of N from the catchment.

occurs. Major melting periods can occur prior to spring snowmelt. In winters when no major melting episodes occurred, the concentration of N in the snowpack remained relatively stable [*Semkin and Jeffries*, 1988]. In contrast, in winters when major melting episodes occurred, N was lost from the snowpack prior to spring snowmelt [*Jeffries and Snyder*, 1981]. We cannot discount the importance of the release of N from the snowpack, but is it enough to contradict the N flushing hypothesis?

The following observations must be considered. First, isotopic studies indicate that, during melting episodes, the contribution of N to discharge waters is dominated by subsurface rather than surface N [*Kendall et al*., 1995; *Shanley and Kendall*, 1995]. *Titus et al*. [1995] suggest that these isotopic studies may even underestimate the contribution of subsurface N, as they observed that, when meltwater flows along its surface flow pathway, there is a mixing of surface and subsurface waters that can result in a substantial flushing of subsurface N during the melting episode. Second, field studies have shown that there is an increase in the concentration of subsurface N during the months leading to spring snowmelt [*Foster*, 1985; *Peters and Driscoll*, 1989; *Yin et al*., 1993]. In catchment 31, for example, in 1986, a year with no major melting episodes within the snowpack and therefore with minimal contributions of N from the snowpack to the soil underneath the snowpack, the concentration of N in the snowpack remained relatively stable at approximately 0.35 mg L^{-1} while the concentration of N in the soil increased from approximately 1.4–2.8 mg L^{-1}, creating a significant reservoir of subsurface N to be flushed. Third, perhaps the strongest evidence of a flushing of subsurface N is that we observe the co-occurrence of flushing activity and N release during high flows in spring snowmelt and during high flows in autumn stormflow and low flows in summer, the latter occurrences not complicated by a surface contribution from snowmelt.

5.5.2. Subsurface unsaturated versus saturated hydrological controls. Our conceptualization of the flushing mechanism is based on the oscillatory dynamics of a saturated throughflow system. During low-*S* conditions, when major portions of the catchment are saturated, this is a reasonable conceptual model. During high-*S* conditions, however, when only minor portions of the catchment are saturated, flushing can occur by partially unsaturated and/or saturated throughflow systems.

During high-*S* conditions, unsaturated flow occurs from upland areas through a system of shallow matrix and/or macropore preferential flow pathways following hydrological events. For example, in the matrix these preferential flow pathways can exist at the interface of soils with differing hydrological properties, including over the hydrophobic organic layer, between organic and mineral layers, or between A and B mineral soil layers. In the macropores these preferential flow pathways can exist along living or dead root systems. The relative contribution of matrix versus macropore flow to the overall subsurface flow is variable and appears to be a function of the soil saturation deficit. *Tsuboyama et al*. [1994] showed that, in a forested catchment with steep slopes and shallow soils, matrix flow dominated discharge waters during all hydrological conditions (i.e., high-*S* to low-*S* conditions). However, as drainage from upland areas increased (i.e., as *S* decreased), the relative contribution to discharge waters from the macropores increased due to the expansion and extension of the macropore networks. Currently, we are not able to distinguish the source of flushing from matrix versus macropore preferential flow pathways from within the catchment. However, based on the study by *Tsuboyama et al*. [1994], optimal conditions for flushing by macropore preferential flow pathways would occur during the wetter, intermediate-*S* conditions rather than the drier, high-*S* conditions. In our study, we did not observe a flushing of N during intermediate-*S* conditions (Figure 18). This observation indicated that the faster macropore preferential flow pathways were not significant conductors of N leaving only the slower matrix preferential flow pathways to conduct N to the discharge waters. We concluded that during high-*S* conditions, flushing from upland areas in the catchment was not a significant process.

During high-*S* conditions, saturated flow is restricted to lowland areas. In catchment 31 we observed that maximum concentrations of N in discharge occurred immediately following the maximum in *S* that occurred during summer droughts (Figure 17). We concluded that flushing occurred by saturated throughflow in the lowland areas, when the soil water content fell below saturation, thereby facilitating a shift in the dominant nitrogen transformation process from denitrification to nitrification and creating a source of N of that could be flushed during the next saturation-generating hydrological event.

While, in catchment 31, flushing by saturated throughflow in lowland areas appears to be an important process, in other areas, flushing by unsaturated throughflow in upland areas may be a more important process. The relative importance of these processes in catchments with distinct hydrological flow pathways needs to be resolved through further model- and field-based studies.

6. Conclusions

The objectives of this paper were to investigate the mechanisms controlling the release of N from catchments and, specifically, to evaluate the role of the flushing hypothesis. Using RHESSys, we developed simple indices for predicting the relative flushing activity within a small headwater catchment. There appear to be two mechanisms for producing significant concentrations of N in catchment discharge waters: (1) a rapid flushing of N when the catchment functions as a source of N to adjacent waters (e.g., during spring snowmelt and autumn stormflow, saturated throughflow rising into previously unsaturated parts of a N-enriched soil profile or, during summer droughts, saturated throughflow rising into previously saturated parts of a N-impoverished soil profile following a period of enhanced rates of nitrification); and (2) a slow draining of N, where N that has been translocated from the bioactive upper layers through matrix or macropore flow pathways to the nonbioactive lower layers of the soil is released over the year or over succeeding years. Although there are two mechanisms, rapid flushing is the dominant mechanism. The results indicate that an understanding of the timing of the catchment N flushing within the transitional states of the catchment as a sink or source area of N to the stream is required and, further, that an understanding of the spatial and temporal heterogeneity of sink and source areas of N within the catchment are important. For prediction of the release of N to the stream, it is not sufficient to predict the hydrological or biogeochemical processes independently. Rather, the interactive impact of these two processes is required.

Future work will focus on refining our conceptual representation of N biogeochemistry by developing algorithms that will enable us to explore the heterogeneity in nitrification and

denitrification processes and patterns within the catchment and their controls on N export.

We are interested in both process-based (represented aspatially) and pattern-based (represented spatially) regulations on the release of N. In examining process-based regulations on N export, we have established that the heterogeneity can be expressed implicitly in the form of an aspatial joint-distribution function of the N source areas, that is, areas where there is a co-occurrence of flushing and source conditions. Although, in this paper, we focused only on the average of the distribution function, in future papers, we will consider the other properties of the distribution function (e.g., skewness, kurtosis, shape). We will determine whether, under a range of catchment conditions, the average is adequate to capture the N export behavior or whether inclusion of the other properties (in particular, the tails of the distribution function, which represent the extremes in the N source areas) will improve the predictive power of the N indices.

In examining pattern-based regulations on N export, we will establish whether inclusion of the spatial properties of the N source areas improves the predictive power of the N indices. Specifically, we will establish whether the N source areas are locationally stable or dynamic, whether they are connected to or disconnected from the stream, and whether they contribute differentially to the export of N from the catchment. These analyses will provide a foundation to examine the emergent behavior of N release among catchments. For example, we will be able to answer the following questions: Do similar distribution functions result in the same N export? and do similar distribution functions with different spatial properties result in the same N export?

The rigor of this simple index approach for predicting the release of N will be tested through its application, initially, to the different catchments in the TLW and, ultimately, to the catchments of regions representing the full range of potential N source and flushing conditions.

Acknowledgments. This research was supported by a NSERCC Doctoral Fellowship and a Tri-Council Eco-Research Doctoral Fellowship to IFC and by support from NSERCC and NASA grants to LEB. We acknowledge the constructive suggestions by the associate editor (J. J. McDonnell) and the reviewers (T. P. Burt and C. P. Cirmo) and an anonymous reviewer which improved the original manuscript. The Turkey Lakes Watershed is operated and supported by Environment Canada and Forestry Canada.

References

Aber, J. D., K. J. Nadelhoffer, P. Steudler, and J. M. Melillo, Nitrogen saturation in northern forest ecosystems, *BioScience*, *39*, 378–386, 1989.

Alexander, M., *Introduction to Soil Microbiology*. 2nd ed., 467 pp., John Wiley, New York, 1977.

Anderson, M. G., and T. P. Burt, The contribution of throughflow to storm runoff: An evaluation of a chemical mixing model, *Earth Surf. Processes Landforms*, *7*, 565–574, 1982.

Band, L. E., Analysis and representation of drainage basin structure with digital elevation data, in *Proceedings of Second International Symposium on Spatial Data Handling*, pp. 437–450, Int. Geogr. Union, Seattle, Wash., 1986.

Band, L. E., A terrain-based watershed information system, *Hydrol. Processes*, *3*, 151–162, 1989.

Band, L. E., Effect of land surface representation on forest water and carbon budgets, *J. Hydrol.*, *150*, 749–772, 1993.

Band, L. E., D. L. Petersen, S. W. Running, J. C. Coughlan, R. B. Lammers, J. Dungan, and R. Nemani, Forest ecosystem processes at the watershed scale: Basis for distributed simulation, *Ecol. Modell.*, *56*, 151–176, 1991.

Band, L. E., P. Patterson, R. Nemani, and S. W. Running, Forest ecosystem processes at the watershed scale: Incorporating hillslope hydrology, *Agric. For. Meteorol.*, *63*, 93–126, 1993.

Baron, J., D. McKnight, and A. S. Denning, Sources of dissolved and particulate organic material in Loch Vale watershed, Rocky Mountain National Park, Colorado, U.S.A., *Biogeochemistry*, *15*, 89–110, 1991.

Berg, B., and H. Staaf, Leaching, accumulation and release of nitrogen in decomposing forest litter, *Ecol. Bull.*, *24*, 43–69, 1981.

Beven, K., Runoff production and flood frequency in catchments of order n: An alternative approach, in *Scale Problems in Hydrology*, edited by V. K. Gupta, I. Rodriguez-Iturbe, E. F. Wood, D. Reidel, pp. 107–131, Norwell, Mass., 1986.

Beven, K., and M. J. Kirkby, A physically based, variable contributing area model of basin hydrology, *Hydrol. Sci. Bull.*, *24*, 43–69, 1979.

Bottomley, D. J., D. Craig, and L. M. Johnston, Neutralization of acid runoff by groundwater discharge to streams in Canadian Precambrian Shield watersheds, *J. Hydrol.*, *75*, 1–26, 1984.

Bottomley, D. J., D. Craig, and L. M. Johnston, Oxygen-18 studies of snowmelt runoff in a small Precambrian Shield watershed: Implications for streamwater acidification in acid-sensitive terrain, *J. Hydrol.*, *88*, 213–234, 1986.

Boyer, E. W., G. M. Hornberger, K. E. Bencala, and D. M. McKnight, Variation of dissolved organic carbon during snowmelt in soil and stream waters of two headwater catchments, Summit County, Colorado, *Biogeochemistry of Seasonally Snow-Covered Catchments*, *IAHS Publ.*, 228, 303–312, 1995.

Boyer, E. W., G. M. Hornberger, K. E. Bencala, and D. McKnight, Overview of a simple model describing variation of dissolved organic carbon in an upland catchment, *Ecol. Modell.*, *86*, 183–188, 1996.

Bristow, K. L., and G. S. Campbell, On the relationship between incoming solar radiation and daily maximum and minimum temperature, *Agric. For. Meteorol.*, *31*, 159–166, 1984.

Canada Soil Survey Committee, Canadian system of soil classification, *Publ. 1646*, 164 pp., Dep. of Agri., Ottawa, 1978.

Carpenter, S. R., S. W. Chisholm, C. J. Krebs, D. W. Schindler, and R. F. Wright, Ecosystem experiments, *Science*, *269*, 324–327, 1995.

Cowell, D. W., and G. M. Wickware, Preliminary analyses of soil chemical and physical properties, Turkey Lakes Watershed, Algoma, Ontario, *Rep. 83-08*, Turkey Lakes Watershed, Algoma, Ontario, Canada, 1983.

Creed, I. F., L. E. Band, I. K. Morrison, J. A. Nicolson, D. S. Jeffries, and R. S. Semkin, Topographic controls on the spatial distribution of nitrogen flows from land to lake systems, *Regional Assessment of Freshwater Ecosystems and Climate Change in North America Symposium*. Leesburg, Va., Oct. 24–26, 1994.

Denning, A. S., J. Baron, M. A. Mast, and M. Arthur, Hydrologic pathways and chemical composition of runoff during snowmelt in Loch Vale watershed, Rocky Mountain National Park, Colorado, U.S.A., *Water Air Soil Pollut.*, *59*, 107–123, 1991.

Dunne, T., and L. B. Leopold, *Water in Environmental Planning*, 818 pp., W. H. Freeman, New York, 1978.

Edwards, A. M. C., The variation of dissolved constituents with discharge in some Norfolk rivers, *J. Hydrol.*, *18*, 219–242, 1973.

Elliot, H., Geophysical survey to determine overburden thickness in selected areas within the Turkey Lakes Watershed basin, Algoma District, Ontario, *Rep. 85-09*, Turkey Lakes Watershed, Algoma, Ontario, Canada, 1985.

Evans, I. S., An integrated system of terrain analysis and slope mapping, *Z. Geomorphol.*, *Suppl.*, *36*, 274–295, 1980.

Federer, C. A., Nitrogen mineralization and nitrification: Depth variation in four New England forest soils, *Soil Sci. Soc. Am. J.*, *47*, 1008–1014, 1983.

Fiebig, D. M., M. A. Lock, and C. Neal, Soil water in the riparian zone as a source of carbon for a headwater stream, *J. Hydrol.*, *116*, 217–237, 1990.

Foster, N. W., Acid precipitation and soil solution chemistry within a maple-birch forest in Canada, *For. Ecol. Manage.*, *12*, 215–231, 1985.

Foster, N. W., Influences of seasonal temperature on nitrogen and sulfur mineralization/immobilization in a maple-birch forest floor in central Ontario, *Can. J. Soil Sci.*, *69*, 501–514, 1989.

Foster, I. D. L., and I. C. Grieve, Short term fluctuations in dissolved organic matter concentrations in streamflow draining a forested

watershed and their relation to the catchment budget, *Earth Surf. Processes Landforms*, *7*, 417–425, 1982.

Foster, N. W., J. A. Nicolson, and P. W. Hazlett, Temporal variation in nitrate and nutrient cations in drainage waters from a deciduous forest, *J. Environ. Qual*., *18*, 238–244, 1989.

Foster, N. W., I. K. Morrison, X. Yin, and P. A. Arp, Impact of soil water deficits in a mature sugar maple forest: stand biogeochemistry, *Can. J. For. Res*., *22*, 1753–1760, 1992.

Galloway, J. N., W. H. Schlesinger, H. Levy II, A. Michaels, and J. L. Schnoor, Nitrogen fixation: Anthropogenic enhancement-environmental response, *Global Biogeochem. Cycles*, *9*, 235–252, 1995.

Garnier, B. J., and A. Ohmura, A method of calculating the direct shortwave radiation income of slopes, *J. Appl. Meteorol*., *7*, 796–800, 1968.

Giblin, P. E., and E. J. Leahy, Geological compilation of the Batchawana sheet, Districts of Algoma and Sudbury, Ontario, *Preliminary Map 302*, Geol. Surv. Can., Ontario, 1977.

Hill, A. R., and M. Shackleton, Soil N mineralization in relation to nitrogen solution chemistry in a small forested watershed, *Biogeochemistry*, *8*, 167–184, 1989.

Hornberger, G. M., K. J. Beven, B. J. Cosby, and D. E. Sappington, Shenandoah Watershed Study: Calibration of a topography-based, variable contributing area hydrological model to a small forested catchment, *Water Resour. Res*., *21*, 1841–1850, 1985.

Hornberger, G. M., K. E. Bencala, and D. M. McKnight, Hydrological controls on dissolved organic carbon during snowmelt in the Snake River near Montezuma, Colorado, *Biogeochemistry*, *25*, 147–165, 1994.

Jeffries, D. S., and R. S. Semkin, Basin description and information pertinent to mass balance studies of the Turkey Lakes Watershed, *Rep. 82-01*, Turkey Lakes Watershed, Algoma, Ontario, Canada, 1982.

Jeffries, D. S., and W. R. Snyder, Variations in the chemical composition of the snowpack and associated meltwaters in central Ontario, in *Proceedings 38th Eastern Snow Conference*, edited by B. E. Goodison, pp. 11–22, Syracuse, N. Y., 1981.

Kelliher, F. M., R. Leuning, M. R. Raupach, and E.-D. Schulze, Maximum conductances for evaporation from global vegetation types, *Agric. For. Meteorol*., *73*, 1–16, 1995.

Kendall, C., D. H. Campbell, D. A. Burns, J. B. Shanley, S. R. Silva, and C. C. Chang, Tracing sources of nitrate in snowmelt runoff using the oxygen and nitrogen isotopic compositions of nitrate, *Biogeochemistry of Seasonally Snow-Covered Catchments*, *IAHS Publ*., *228*, 339–347, 1995.

Klein, T. M., J. P. Kreitinger, and M. Alexander, Nitrate formation in acid forest soils from the Adirondacks, *Soil Sci. Soc. Am. J*., *47*, 506–508, 1983.

Krause, H. H., Nitrate formation and movement before and after clear-cutting of a monitored watershed in central New Brunswick, Canada, *Can. J. For. Res*., *12*, 922–930, 1982.

Lammers, R. B., and L. E. Band, Automating object representation of drainage basins, *Comp. Geosci*., *16*, 787–810, 1990.

Lewis, W. M., Jr., and M. C. Grant, Relationships between stream discharge and yield of dissolved substances from a Colorado Mountain watershed, *Soil Sci*., *128*, 353–363, 1979.

Lohammer, T., S. Larron, S. Linder, and S. O. Falk, FAST_Simulation models of gaseous exchange in Scots pine, *Structure and Function of Northern Coniferous Forests—An Ecosystem Study*, *Ecol. Bull*., *32*, 505–523, 1980.

Mackay, D. S., and L. E. Band, Extraction and representation of watershed structure including lakes and wetlands from digital terrain and remote sensing information, *Eos Trans. AGU*, *75*, Spring Meet. Suppl., S175, 1994.

McDonnell, J. J., A rationale for old water discharge through macropores in a steep, humid catchment, *Water Resour. Res*., *26*, 2821–2832, 1990.

Mollitor, A. V., and D. J. Raynal, Acid precipitation and ionic movements in Adirondack forest soils, *Soil Sci. Soc. Am. J*., *46*, 137–141, 1982.

Monteith, J. L., Evaporation and environment, *Sym. Soc. Exp. Biol*., *19*, 205–234, 1965.

Morrison, I. K., Effect of trap dimensions on mass of litterfall collected in an *Acer saccharum* stand in northern Ontario, *Can. J. For. Res*., *21*, 939–931, 1985.

Morrison, I. K., N. W. Foster, and P. W. Hazlett, Carbon reserves, carbon cycling and harvesting effects in three mature forest types in Canada, *N. Z. J. For. Sci*., *23*, 403–412, 1993.

Mulholland, P. J., Regulation of nutrient concentrations in a temperate forest stream: Roles of upland, riparian, and instream processes, *Limnol. Oceanogr*., *37*, 1512–1526, 1992.

Murdoch, P. S., and J. L. Stoddard, The role of nitrate in the acidification of streams in the Catskill Mountains of New York, *Water Resour. Res*., *28*, 2707–2720, 1992.

Murray, F. W., On the computation of saturation vapor pressure, *J. Appl. Meteorol*., *6*, 203–204, 1967.

Nemani, R., L. Pierce, S. Running, and L. Band, Forest ecosystem processes at the watershed scale: Sensitivity to remotely-sensed leaf area index measurements, *Int. J. Remote Sens*., *14*, 2519–2534, 1993.

Nicolson, J. A., Water and chemical budgets for terrestrial basins at the Turkey Lakes Watershed, *Can. J. Fish. Aquat. Sci*., *45*, suppl. 1, 88–95, 1988.

Nicolson, J. A., Ion movement in terrestrial basins in the Turkey Lakes Forest Watershed, *Proceedings of Acid Rain and Forest Resources Conference*, *Rep. DPC-X-35*, pp. 526–531, For. Can. Info, Ottawa, 1991.

Parkinson, D., and E. Coups, Microbial activity in a podzol, in *Soil Organisms*, edited by J. Doeksen and J. van der Drift, pp. 167–175, North Holland, New York, 1963.

Parton, W. J., D. S. Schimel, C. V. Cole, and D. S. Ojima, Analysis of factors controlling soil organic matter levels in Great Plains grasslands, *Soil Sci. Soc. Am. J*., *51*, 1173–1179, 1987.

Peters, N. E., and C. T. Driscoll, Sources of acidity during snowmelt at a forested site in the west-central Adirondack Mountains, New York, *IAHS Publ*., *167*, 99–108, 1987.

Peters, N. E., and C. T. Driscoll, Temporal variations in solute concentrations of meltwater and forest floor leachate at a forested site in the Adirondacks, New York, in *Proceedings of 46th Eastern Snow Conference*, pp. 45–56, Quebec City, Quebec, Canada, 1989.

Peters, D. L., J. M. Buttle, C. H. Taylor, and B. D. LaZerte, Runoff production in a forested, shallow soil, Canadian Shield basin, *Water Resour. Res*., *31*, 1291–1304, 1995.

Press, W. H., B. P. Flannery, S. A. Teukolsky, and W. T. Vetterling, *Numerical Recipes in C—The Art of Scientific Computing*, 735 pp., Cambridge Univ. Press, New York, 1988.

Rascher, C. M., C. T. Driscoll, and N. E. Peters, Concentrations and flux of solutes from snow and forest floor during snowmelt in the west-central Adirondack region of New York, *Biogeochemistry*, *3*, 209–224, 1987.

Robson, A., and C. Neal, Chemical signals in an upland catchment in mid-Wales—some implications for water movement. *Third National Hydrology Symposium*, pp. 3.17–3.24, Br. Hydrol. Soc., Oxon, England, 1991.

Robson, A., K. Beven, and C. Neal, Towards identifying sources of subsurface flow: A comparison of components identified by a physically based runoff model and those determined by chemical mixing techniques, *Hydrol. Processes*, *6*, 199–214, 1992.

Running, S. W., and J. C. Coughlan, A general model of forest ecosystem processes for regional applications, I, Hydrologic balance, canopy gas exchange and primary production processes, *Ecol. Modell*., *42*, 125–154, 1988.

Running, S. W., and S. T. Gower, FOREST-BGC, A general model of forest ecosystem processes for regional application, II, Dynamic carbon allocation and nitrogen budgets, *Tree Physiol*., *9*, 147–160, 1991.

Running, S. W., and E. R. Hunt Jr., Generalization of a forest ecosystem process model for other biomes, BIOME-BGC, and an application for global-scale models, in *Scaling Physiological Processes: Leaf to Globe*, edited by J. R. Ehleringer and C. B. Field, pp. 141–158, Academic, San Diego, Calif., 1993.

Running, S. W., R. R. Nemani, and R. D. Hungerford, Extrapolation of synoptic meteorological data in mountainous terrain and its use for simulating forest evapotranspiration and photosynthesis, *Can. J. For. Res*., *17*, 472–483, 1987.

Schaefer, D. A., and C. T. Driscoll, Identifying sources of snowmelt acidification with a watershed mixing model, *Water Air Soil Pollut*., *67*, 345–365, 1993.

Semkin, R. G., and D. S. Jeffries, Storage and release of major ionic contaminants from the snowpack in the Turkey Lakes Watershed, *Water Air Soil Pollut*., *31*, 215–221, 1986.

Semkin, R. G., and D. S. Jeffries, Chemistry of atmospheric deposition,

the snowpack, and snowmelt in the Turkey Lakes Watershed, *Can. J. Fish. Aquat. Sci*., *45*, suppl. 1, 38–46, 1988.

Semkin, R. G., D. S. Jeffries, and R. Neureuther, Relationships between hydrological conditions and the ionic composition of streamwaters in the Turkey Lakes Watershed, in *Proceedings of Canadian Hydrological Symposium*, *Publ. 24633*, pp. 109–122, Natl. Res. Council of Can., Ottawa, 1984.

Shanley, J. B., and C. Kendall, Hillslope hydrochemistry and the streamwater response during snowmelt, *Eos Trans. AGU*, *75*, Spring Meet. Suppl., S111, 1995.

Shepard, J. P., M. J. Mitchell, and T. J. Scott, Soil solution chemistry of an Adirondack Spodosol: Lysimetry and N dynamics, *Can. J. For. Res*., *20*, 818–824, 1990.

Sirois, A., and R. J. Vet, Detailed analysis of sulphate and nitrate atmospheric deposition estimates at the Turkey Lakes Watershed, *Can. J. Fish. Aquat. Sci*., *45*, suppl. 1, 14–25, 1988.

Stoddard, J. L., Long-term changes in watershed retention of nitrogen: Its causes and aquatic consequences, in *Environmental Chemistry of Lakes and Reservoirs*, edited by L. A. Baker, pp. 223–282, Am. Chem. Soc., Washington, D. C., 1994.

Titus, A. C., J. J. McDonnell, J. Shanley, and C. Kendall, Snowmelt runoff production in a small forested catchment: A combined hydrometric and isotopic tracing approach, *Eos Trans. AGU*, *76*, Fall Meet. Suppl., F216, 1995.

Tsuboyama, Y., R. C. Sidle, S. Noguchi, and I. Hosoda, Flow and solute transport through the soil matrix and macropores of a hillslope segment, *Water Resour. Res*., *30*, 879–890, 1994.

Van Miegroet, H., D. W. Cole, and N. W. Foster, Nitrogen chemistry, deposition, and cycling in forests [Nitrogen distribution and cycling], in *Atmospheric Deposition and Forest Nutrient Cycling: A Synthesis of the Integrated Forest Study*, edited by D. W. Johnson and S. E. Lindberg, pp. 178–196, Springer-Verlag, New York, 1992.

Vitousek, P. M., and W. A. Reiners, Ecosystem succession and nutrient retention, a hypothesis, *BioScience*, *25*, 376–381, 1975.

Walling, D. E., Suspended sediment and solute yields from a small catchment prior to urbanization, *Fluvial Processes in Instrumented Watersheds*, *Inst. Brit. Geogr. Spec. Publ*., *6*, 169–192, 1974.

Walling, D. E., and I. D. L. Foster, Variations in the natural chemical concentration of river water during flood flows, and the lag effect: Some further comments, *J. Hydrol*., *26*, 237–244, 1975.

Wang, F. L., and J. R. Bettany, Influence of freeze-thaw and flooding on the loss of organic carbon and carbon dioxide from soil, *J. Environ. Qual*., *22*, 709–714, 1993.

Wang, F. L., and J. R. Bettany, Organic and inorganic nitrogen leaching from incubated soils subjected to freeze-thaw and flooding conditions, *Can. J. Soil Sci*., *74*, 201–206, 1994.

Wolock, D. M., G. M. Hornberger, and T. J. Musgrove, Topographic effects on flow path and surface water chemistry of the Llyn Brianne catchments in Wales, *J. Hydrol*., *115*, 243–259, 1990.

Yin, X., N. W. Foster, and P. A. Arp, Solution concentrations of nutrient ions below the rooting zone of a sugar maple stand: relations to soil moisture, temperature, and season, *Can. J. For. Res*., *23*, 617–624, 1993.

L. E. Band and I. F. Creed, Department of Geography, University of Toronto, 100 St. George Street, Toronto, Ontario, Canada M5S 3G3. (e-mail: creed@geog.utoronto.ca)

N. W. Foster, I. K. Morrison, and J. A. Nicolson, Forestry Canada, Great Lakes Forestry Centre, Sault Ste. Marie, Ontario, Canada P6A 5M7.

D. S. Jeffries and R. S. Semkin, Environment Canada, Canada Centre for Inland Waters, Burlington, Ontario, Canada L7R 4A6.

(Received November 27, 1995; revised July 25, 1996;
accepted August 2, 1996.)